

# Towards a worldsheet theory of entanglement entropy

Houwen Wu and Shuxuan Ying

*College of Physics  
Sichuan University  
Chengdu, 610065, China*

*Department of Physics  
Chongqing University  
Chongqing, 401331, China*

iverwu@scu.edu.cn, ysxuan@cqu.edu.cn

## Abstract

We propose a new action for entanglement entropy in the framework of the  $\text{AdS}_3/\text{CFT}_2$  correspondence. This action is constructed directly from the entanglement entropy of the  $\text{CFT}_2$ , and we show that the Einstein equations of  $\text{AdS}_3$  gravity can be derived from it. In the near-coincidence limit, using Riemann normal coordinates, the action reduces to a string worldsheet action in a curved background that naturally includes the symmetric spacetime metric, an antisymmetric Kalb-Ramond field, and a dilaton. The Kalb-Ramond field gives rise to a string charge density, from which we demonstrate that bit threads can be exactly reproduced. This correspondence provides a clear physical interpretation of bit threads. Exploiting this correspondence, we establish explicit relations between the emergent string worldsheet and the Ryu-Takayanagi (RT) surface, providing new insights into entanglement entropy. In particular, entanglement entropy can be computed from open string charge, while Bekenstein-Hawking entropy arises from closed string charge through open-closed string duality. These results suggest a unified picture in which the Susskind-Uglum conjecture, open-closed string duality, and the ER=EPR proposal emerge as equivalent manifestations of the same underlying principle. Finally, we propose a quantization of the RT surface, pointing to a possible connection with loop quantum gravity that refines Wall's conjecture.

## Contents

<b>1</b>	<b>Introduction</b>	<b>2</b>
<b>2</b>	<b>Motivation</b>	<b>10</b>
<b>3</b>	<b>The worldsheet action for entanglement entropy</b>	<b>14</b>
<b>4</b>	<b>Kalb-Ramond charge density as bit threads</b>	<b>23</b>
4.1	Set-up . . . . .	25
4.2	Deriving bit threads in string theory . . . . .	28
4.3	Correspondence between string theory and entanglement entropy . . . . .	33
<b>5</b>	<b>Novel results</b>	<b>35</b>
5.1	Computing entanglement entropy from open string charge . . . . .	35
5.2	Computing Bekenstein-Hawking entropy from closed string charge . . . . .	36
5.3	ER=EPR from the string perspective . . . . .	39
5.4	New realization of Susskind and Uglum's conjecture . . . . .	41
5.5	Are the entanglement entropy and RT surface quantized? . . . . .	44
<b>6</b>	<b>Conclusion and discussion</b>	<b>48</b>

## 1 Introduction

The black hole information paradox remains a central problem in modern theoretical physics. A significant development in this context was the work of Ryu and Takayanagi, who established a relationship between the entanglement entropy (specifically, the von Neumann entropy) in two-dimensional conformal field theory (CFT<sub>2</sub>) and the area of extremal surfaces—known as Ryu-Takayanagi (RT) surfaces—in the bulk of AdS<sub>3</sub> [1, 2, 3]. Building on this result, one can compute the von Neumann entropy of gravitational systems via the quantum extremal surface prescription [4, 5]. This approach has been successfully applied to evaporating black holes and their associated Hawking radiation, yielding results consistent with the Page curve [6, 7]. Nevertheless, the precise quantum state corresponding to the entanglement entropy of Hawking radiation remains unclear, posing a key unresolved aspect of the information paradox [8].

Susskind and Uglum proposed that black hole entropy could be derived from the closed string worldsheet, where the string sphere is punctured twice by the black hole horizon, as illustrated in the

left panel of figure (1) [9]. This picture can also be interpreted from the open string perspective, in which the string endpoints are fixed on the horizon. In this framework, a slice of the closed string (the sphere) intersecting the horizon appears as an open string to a Rindler observer outside the event horizon (right panel of figure (1)), offering a statistical interpretation of entanglement entropy. Susskind and Uglum's conjecture thus suggests that both black hole entropy and entanglement entropy can be computed in string theory, potentially allowing the identification of their underlying quantum states. Recently, Ahmadain and Wall provided a proof of the closed string version of this conjecture using the sphere diagram in off-shell closed string theory, reproducing the expected result  $\text{Area}/4G_N$  [10, 11, 12]. However, establishing the open string version remains challenging, as the replica trick introduces a conical singularity that breaks the conformal symmetry of the string worldsheet.

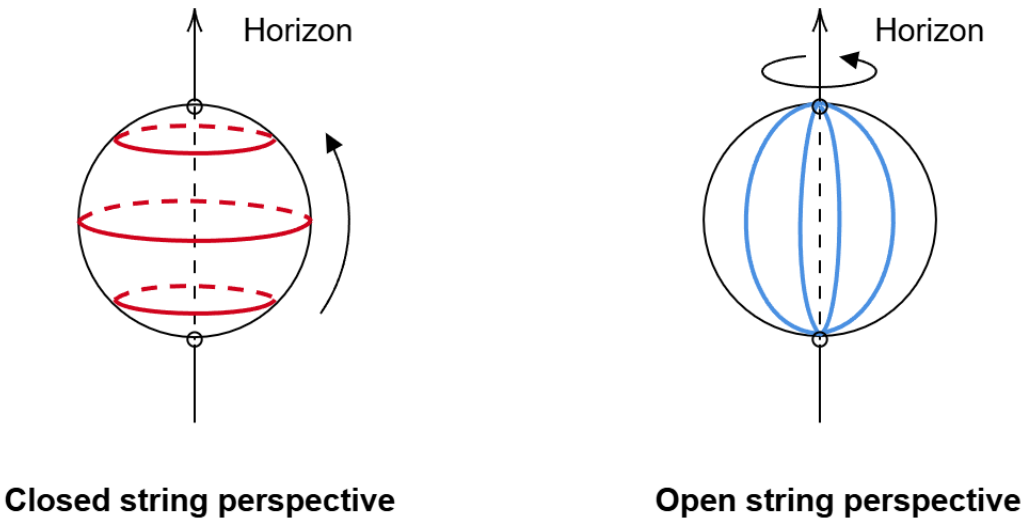


Figure 1: The left panel of the figure illustrates the closed string perspective in the Susskind and Uglum's setup. The blue circle represents a closed string whose initial and final states interact with the event horizon. In contrast, the right panel depicts the open string configuration, indicated by the red lines, with endpoints fixed on the horizon. In this case, the target space naturally factorizes into two Hilbert spaces corresponding to the open strings inside and outside the event horizon:  $\mathcal{H} \subseteq \mathcal{H}_{out} \otimes \mathcal{H}_{in}$ . This factorization provides a statistical interpretation of entanglement entropy, as discussed in [11].

If Susskind and Uglum's conjecture is correct, there must exist a correspondence between the string worldsheet and the RT surface. Such a correspondence could plausibly serve as a guiding principle for developing the open string perspective of the conjecture in the framework of bosonic string theory, ultimately enabling the computation of entanglement entropy using the string worldsheet. With this framework in place, the black hole information paradox can be revisited from a new perspective, potentially revealing the microscopic quantum state of Hawking radiation. In previous works, qualitative evidence for a relationship between the string worldsheet and the RT surface has been found in both

open and closed string field theories [13, 14]. Both entanglement entropy and string field theory are fundamentally grounded in hyperbolic geometry. Furthermore, key dynamical features—such as phase transitions in the entanglement wedge cross section (EWCS) [15] or reflected surface [16], and the Batalin–Vilkovisky (BV) master equations in open or closed string field theory [17, 18]—appear to be intrinsically linked. These observations suggest that the correspondence is not a mere coincidence due to shared geometric structures but reflects a deeper, underlying connection. Nevertheless, a rigorous quantitative proof of this correspondence remains elusive. A similar observation was recently made in [19]: as expected, the RT surface for multiboundary black holes—which in our framework corresponds to the string vertices discussed earlier—can be derived directly from the dual  $CFT_2$ .

Moreover, there are several related approaches to computing entanglement entropy using string theory. The first method involves evaluating the entropy in string theory via orbifolds [20, 21, 22, 23, 24], where the orbifold fixed point corresponds to the tip of a cone with opening angle  $\beta = 2\pi/N$ . However, the methods in [22, 23, 24] face a notable difficulty: they fail to reproduce the entropy in the  $N = 1$  limit, which is required for consistency with the Susskind–Uglum conjecture. On the other hand, as emphasized in [11], another approach [25, 26] suffers from a conceptual issue. In this approach, the “position” of a string is defined solely by the location of its center of mass. However, due to string vibrations, different parts of the string can extend outside the assigned region, making the center-of-mass prescription inconsistent with the actual spatial support of the string.

In this paper, *rather than pursuing a bottom-up strategy that attempts to collect and synthesize fragmented evidence from various theoretical frameworks, we adopt a top-down approach*. Specifically, we aim to reformulate the theory of entanglement entropy directly in the framework of  $AdS_3/CFT_2$  correspondence. In other words, we directly propose an action for entanglement entropy and demonstrate that it reduces to the string worldsheet action in curved spacetime. This approach yields an explicit and quantitative relation between the string worldsheet and the RT surface. To approach this aim, we begin by observing that the entanglement entropy in  $CFT_2$  corresponds to the geodesic length  $L(X, X')$  in  $AdS_3$ :

$$S_{vN}(A : B) = \frac{L(X, X')}{4G_N^{(3)}}, \quad (1)$$

where  $G_N^{(3)}$  is a three-dimensional Newton’s constant. From this geodesic length, we can extract Syng’s world function [27], which can be expressed in terms of the entanglement entropy as

$$\Omega(X, X') = \frac{1}{2}L(X, X')^2 = 8 \left[ G_N^{(3)} S_{vN}(A : B) \right]^2. \quad (2)$$

We define the partial derivatives of  $\Omega$  with respect to  $X$  and  $X'$  as  $\Omega_\mu := \partial\Omega/\partial X^\mu$  and  $\Omega_{\mu'} := \partial\Omega/\partial X^{\mu'}$ , respectively. The covariant derivative of  $\Omega_\mu$  with respect to  $X$  is denoted as  $\Omega_{\mu\nu} := \nabla_\nu \Omega_\mu$ , while the mixed derivative with respect to  $X'$  is  $\Omega_{\mu\nu'} := \partial_{\nu'} \Omega_\mu$ . An important concept in this context is the coincidence limit, in which  $X' \rightarrow X$ , denoted by  $[\dots]$ . Under this limit, the spacetime metric derived from the geodesic length is given by

$$g_{\mu\nu}(X) = -[\Omega_{\mu\nu}] = -\lim_{X' \rightarrow X} \partial_\mu \partial_{\nu'} \Omega(X, X') , \quad g_{\mu\nu}(X) = [\Omega_{\mu\nu}] = \lim_{X' \rightarrow X} \nabla_\nu \partial_\mu \Omega(X, X') . \quad (3)$$

To retain more geometric information, we can consider the **near-coincidence** limit  $X \rightarrow X'$  [28], yielding the expansion:

$$\Omega_{\mu'\nu'}(X, X') = g_{\mu'\nu'}(X') - \frac{1}{3} R_{\mu'\lambda'\nu'\kappa'}(X) \Omega^{\lambda'}(X, X') \Omega^{\kappa'}(X, X') + \dots \quad (4)$$

This expression closely parallels the expansion of the closed string worldsheet action in Riemann normal coordinates (RNC).

Here, a key insight emerges. In string theory, gravity is known to arise from CFT. When a string propagates in a curved background, the requirement that the worldsheet theory remain conformally invariant at the quantum level imposes constraints on the background geometry—namely, the string-theoretic version of the Einstein equations [29]. This observation raises a compelling question: can we apply the same logic to entanglement entropy using the expansion of  $\Omega_{\mu'\nu'}$ ? More precisely, can we impose conformal symmetry on this expansion and derive Einstein equations? This question is well-motivated, especially since  $\Omega_{\mu'\nu'}$ , which encodes geometric data such as the geodesic separation between two points in spacetime, is entirely constructed from CFT correlators. If  $\Omega_{\mu'\nu'}$  arises from CFT, then requiring quantum-level conformal invariance may indeed constrain the emergent geometry—potentially leading to gravitational dynamics from entanglement itself.

Fortunately, a natural scalar quantity is already available: the Synge's world function  $\Omega(X, X')$ , derived from entanglement entropy, which can serve as the foundation for constructing an action. This function satisfies the identity

$$2\Omega = g_{\mu\nu}(X) \Omega^\mu \Omega^\nu = \Omega_{\mu\nu} \Omega^\mu \Omega^\nu , \quad (5)$$

suggesting that the dynamics of entanglement may be governed by an action analogous to that of a point particle or a string worldsheet. The Synge's world function, defined as half the squared geodesic distance between two bulk points  $X$  and  $X'$ , is computable from the  $\text{CFT}_2$  and naturally depends on the  $\text{CFT}_2$  coordinates  $(\tau, \sigma)$ . While a single geodesic corresponds to the minimal RT surface anchored on a boundary interval, varying the entangling region continuously generates a family of geodesics that collectively sweep out a two-dimensional surface in the bulk. This motivates parameterizing the non-local action as

$$S_E = \frac{1}{\ell^2} \int d^2 \sigma' \Omega_{\mu'\nu'} \partial_{\alpha'} \Omega^{\mu'} \partial^{\alpha'} \Omega^{\nu'} , \quad \alpha' = (\tau', \sigma') . \quad (6)$$

where  $\ell$  denotes a characteristic length scale. We use the prime notation here because, by expanding the action in the near-coincidence limit  $X \rightarrow X'$ <sup>1</sup> and employing RNC  $\mathbb{X}$ , we obtain

---

<sup>1</sup>Since  $X$  and  $X'$  are interchangeable, one may also drop the prime in the action (6) and take the limit  $X' \rightarrow X$ .

$$S_E = \int d^2\sigma \left( g_{ab} \partial_\alpha \mathbb{X}^a \partial^\alpha \mathbb{X}^b - \frac{\ell^2}{3} R_{acbd} \mathbb{X}^c \mathbb{X}^d \partial_\alpha \mathbb{X}^a \partial^\alpha \mathbb{X}^b + \dots \right), \quad (7)$$

which is precisely the string worldsheet action in a curved background. Thus, in the near-coincidence limit, the expansion of  $\Omega(X, X')$  yields, at leading order, a local quadratic action equivalent to the Polyakov kinetic term for the small separation field  $\mathbb{X}^a$ . Locally, the effective dynamics of geodesic fluctuations is therefore identical to a string worldsheet theory, with curvature corrections provided by higher-order terms. The worldsheet boundary conditions then reduce—under the usual Dirichlet/Neumann split and static gauge—to the target-space geodesic equation governing the embedding of the boundary curve. In this sense, the geodesic is recovered as the image of a specific worldsheet boundary curve, while the worldsheet itself emerges as the two-dimensional surface parametrizing the entire family of geodesics.

However, this action is incomplete. Its corresponding  $\beta$ -function of  $g_{ab}$  does not yield an Einstein's equations that admits  $\text{AdS}_3$  as a solution, which contradicts the foundational assumption that  $\Omega$  originates from the geodesic length in  $\text{AdS}_3$ . To resolve this inconsistency, the theory must be supplemented by an antisymmetric tensor field  $B_{ab}$  (the Kalb–Ramond field) and a constant dilaton  $\phi$ , in addition to the symmetric metric  $g_{ab}$ . The inclusion of  $B_{ab}$  is essential for capturing the full gravitational dynamics of the background, especially those consistent with string theory and  $\text{AdS}_3$  geometry. Given that entanglement entropy is associated with the spacetime metric  $g_{ab}$ , it is natural to expect that there exists a corresponding entanglement-related quantity sourced by the Kalb–Ramond field  $B_{ab}$ . To identify this quantity, let us recall the physical role of the Kalb–Ramond field in string theory. It describes a macroscopic string carrying Kalb–Ramond charge, propagating in the background and interacting with background fields [30, 31, 32]. The corresponding equation of motion is given by:

$$\frac{\partial H^{abc}}{\partial x^c} = \kappa^2 j^{ab}. \quad (8)$$

where the Kalb–Ramond charge density vector is given by  $\vec{j}^0 \equiv j^{0a}$ . This current is divergenceless. Moreover, since we are working in the  $\text{AdS}_3/\text{CFT}_2$  correspondence, the bulk gravity is weak, i.e.  $\kappa^2 = 8\pi G_N^{(3)} \rightarrow 0$ . To ensure that these string sources do not backreact on the  $\text{AdS}_3$  metric at leading order, we must include a constant dilaton  $\phi = \phi_0$  in the action. This yields a weak string coupling  $g_s = \exp(\phi_0) \ll 1$ . Consequently, all three massless sectors of the closed string—the spacetime metric  $g_{ab}$ , the Kalb–Ramond field  $B_{ab}$ , and the dilaton  $\phi$ —are indispensable for establishing the correspondence between the string worldsheet theory and entanglement entropy. On the other hand, in the context of holographic entanglement, a natural candidate for such a divergenceless vector already exists: the bit threads, which represent the flow of entanglement entropy across the RT surface [33]. This suggests the possibility of a direct identification between the string charge density  $\vec{j}^0$  and the bit-thread vector  $v$ . To test this proposal, we first highlight three key properties of  $\vec{j}^0$ :

1.  $\vec{j}^0$  arises from string sources carrying Kalb–Ramond charge and interacting with background fields. A convenient description employs the static gauge, in which the current flows along a single spacetime direction.

2.  $\vec{j}^0$  is localized along a line in spacetime, being proportional to a delta function. To make contact with bit threads, which are continuous vector fields, we must consider an ensemble of multiple parallel open strings.
3. At the string endpoints,  $\vec{j}^0$  reduces to the unit normal vector  $\vec{n}$  on the D-brane. This D-brane plays the role of the RT surface in the bit-thread formulation.

These three features motivate us to place multiple parallel open strings on a time slice of  $\text{AdS}_3$ . The main challenges are (i) how to impose the static gauge on this time slice, and (ii) how to arrange the corresponding D-brane along the geodesic representing the RT surface. Both issues are resolved by considering the BTZ black brane geometry, which can be obtained by introducing multiple string sources in the limits  $\kappa^2 = 8\pi G_N^{(3)} \rightarrow 0$  and  $g_s \ll 1$ :

$$dS_{\pm}^2 = \frac{l_{\text{AdS}}^2}{z_{\pm}^2} \left( -\left(1 - (z_{\pm}/b)^2\right) dt^2 + \frac{dx_{\pm}^2}{1 - (z_{\pm}/b)^2} + dz_{\pm}^2 \right). \quad (9)$$

In this background, we introduce two sets of parallel open strings: set 1 stretches along the  $z_+$ -direction from  $z_+ = b$  to 0, while set 2 stretches along the  $z_-$ -direction from  $z_- = 0$  to  $b$ , as illustrated in figure (2). The string endpoints (D-branes) naturally sit at  $z_+ = z_- = b$ , corresponding to the planar horizon

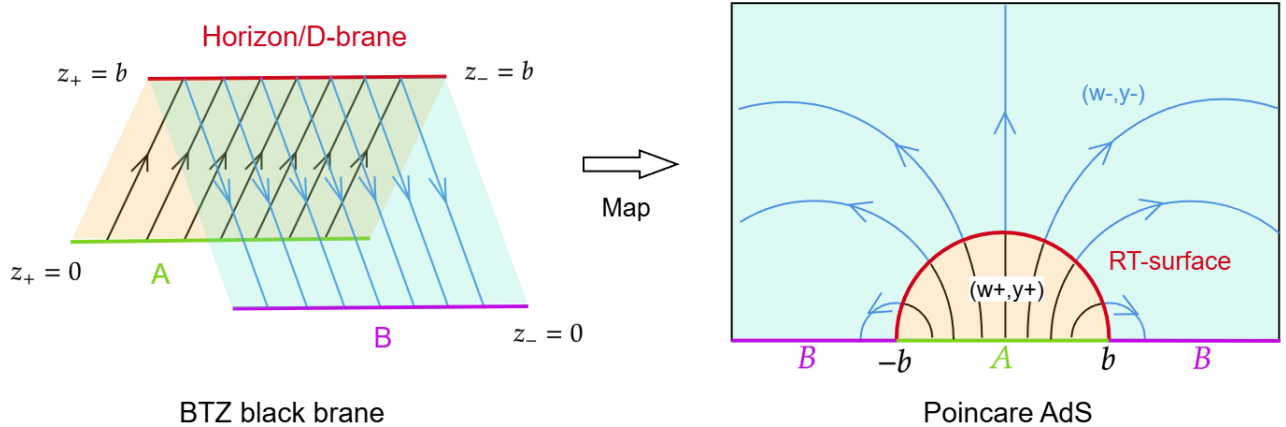


Figure 2: The left-hand panel illustrates two sets of parallel open strings stretched along the  $z_+$ - and  $z_-$ -directions in two copies of the BTZ black brane geometry. The red line at  $z_+ = z_- = b$  represents the planar horizon, or equivalently the D-brane, since the open strings terminate on it. When the two sets of parallel open strings uniformly cover the horizon, the number and locations of strings on both sides coincide, allowing them to be smoothly connected. After performing the appropriate coordinate transformation, we obtain the charge density vector in the familiar Poincaré patch of a time slice of  $\text{AdS}_3$ , as shown in the right-hand panel. In this picture, the red D-brane naturally extends along the RT surface, making the correspondence with bit threads manifest. In both panels, the arrows indicate the direction of the charge density vector.

of the BTZ black brane. Because the parallel strings carry Kalb–Ramond charge, when they uniformly

cover the horizon the two sets of strings can be smoothly connected, ensuring that the charge density vector  $\vec{j}^0$  remains divergenceless despite the presence of the horizon. By performing an appropriate coordinate transformation [34, 35, 36], these two sets of open strings map onto two regions of the Poincaré patch of a time slice of  $\text{AdS}_3$ :  $dS_\pm^2 = \frac{l_{\text{AdS}}^2}{w_\pm^2} (dy_\pm^2 + dw_\pm^2)$ . Under this mapping, the D-brane precisely aligns with the geodesic that defines the RT surface. In other words, this  $D$ -brane thus plays the role of the entangling surface, or more precisely, the entangling brane ( $E$ -brane) [37]. From this construction, we can obtain the vector field from string theory

$$v = \frac{l_{\text{AdS}}}{2G_N^{(3)}} \vec{j}^0 = \frac{1}{4G_N^{(3)}} \frac{1}{l_{\text{AdS}}} \left( \frac{2bw}{\sqrt{(b^2 - y^2 - w^2)^2 + 4b^2w^2}} \right)^2 \left( \frac{b^2 - y^2 + w^2}{2b}, \frac{yw}{b} \right), \quad (10)$$

which coincides precisely with the bit threads. This provides evidence for a possible correspondence between the string worldsheet and the RT surface: the Kalb–Ramond charge density vector  $\vec{j}^0$  maps directly to the bit-thread vector  $v$ . Furthermore, the D-brane extends along a geodesic in the  $\text{AdS}_3$  time slice, corresponding to the RT surface of the entangling region.

This correspondence provides a new framework to calculate and understand the origin of entanglement entropy. The entanglement entropy can be computed by counting the number  $\mathcal{N}$  of open strings—each carrying Kalb–Ramond charge—that intersect the entangling surface:

$$S_{\text{vN}} = \frac{L_{\gamma_A}}{4G_N^{(3)}} = \frac{l_{\text{AdS}}}{4G_N^{(3)}} \cdot 2\mathcal{N} = \frac{c}{3} \ln \left( \frac{2b}{\epsilon} \right), \quad (11)$$

where  $2b$  denotes the length of the interval corresponding to the entangling region  $A$ , as illustrated in (2). This interpretation provides a microscopic, string-theoretic origin for entanglement entropy, where each charged open string contributes a discrete unit of information. By open–closed string duality, the open string charge transforms into a closed string charge. Since the corresponding closed string winds around the horizon and is non-contractible, its total charge is non-vanishing and is given by

$$Q = 2\pi r, \quad (12)$$

where  $r$  is the horizon radius. Consequently, the Bekenstein–Hawking entropy follows as

$$S_{\text{BH}} = \frac{Q}{4G_N^{(3)}} = \frac{2\pi r}{4G_N^{(3)}}, \quad (13)$$

which exactly reproduces the BTZ black hole entropy. This result verifies the Susskind–Uglum conjecture within the  $\text{AdS}_3/\text{CFT}_2$  framework: open strings contribute to entanglement entropy, while closed strings contribute to black hole entropy. Furthermore, it demonstrates that the two-punctured spheres of the original Susskind–Uglum construction are replaced by hyperbolic cylinders in  $\text{AdS}_3$ . The open–and closed–string descriptions extend naturally to this cylinder geometry. In this realization, the entangling surface or horizon, which punctures the two-sphere in the original setup, is identified with the waist of the hyperbolic cylinder in  $\text{AdS}_3$ , corresponding to the throat of the wormhole.

Building on this new perspective, we obtain a string-theoretic interpretation of  $\text{ER} = \text{EPR}$ . In this picture, the closed string winds around the wormhole horizon, with its winding charge directly accounting for the Bekenstein–Hawking entropy. As the entanglement entropy between subsystems  $A$  and  $B$  decreases, the bulk horizon shrinks. When the horizon radius falls below the string length scale, the winding closed string develops tachyonic modes. This triggers closed string tachyon condensation, reducing the total winding charge  $Q$  to zero. The vanishing of  $Q$  implies that the closed string winding around the compactified dimension becomes contractible, signaling that the originally connected spacetime with a finite compact dimension splits into two disconnected components.

All of these observations suggest that open–closed string duality,  $\text{ER} = \text{EPR}$ , and the Susskind–Uglum conjecture are not merely analogous but represent manifestations of a deeper equivalence. In all three frameworks, the transition between dual descriptions—whether in string theory, spacetime geometry, or entanglement entropy—reflects the same underlying principle.

Finally, instead of considering multiple parallel open strings carrying Kalb–Ramond charge—each contributing to the entanglement entropy—we now restrict to a finite number of strings. In this case, the entanglement entropy becomes discretized according to the number of strings, providing strong evidence that the RT surface itself should be quantized. In the continuum limit,  $\mathcal{N} \rightarrow \infty$  with inter-string spacing  $d_s \rightarrow 0$ , the system effectively approaches a continuous description, and the result reduces to the well-known  $\text{CFT}_2$  entanglement entropy. In our picture, an oriented open string intersected by the RT surface is divided into two segments, and the entanglement entropy naturally measures the quantum correlations between these two parts. This structure closely parallels loop quantum gravity (LQG), where the entangling surface cuts an oriented Wilson line state  $\gamma$  into two parts, and the entanglement entropy between them is quantized, yielding discrete values. This analogy suggests a potential bridge between string theory and LQG, realized through the discrete nature of entanglement entropy. More concretely, by performing a Schmidt decomposition of both the open string charge density and the LQG Wilson line, one can split each system into two parts and then recombine halves to form a new configuration. Since both descriptions share the same quantized wormhole horizon, and because oriented open strings can attach to oriented Wilson lines at the same points on the horizon, the two theories must coincide on the wormhole throat. This observation resonates with Wall’s conjecture, suggesting that the wormhole throat could provide a possible framework where string theory and LQG exhibit a deep connection through entanglement between the string CFT and the LQG CFT [38].

This paper is organized as follows. In Section 2, we outline the motivation, showing how Einstein equations can emerge from  $\text{CFT}_2$  through string theory and arguing that entanglement entropy possesses a closely related structure. Section 3 constructs an action directly from the entanglement entropy of  $\text{CFT}_2$ . In the near-coincidence limit and Riemann normal coordinates, this effective action reduces to the string worldsheet action in curved spacetime. To ensure that the emergent gravity is  $\text{AdS}_3$ , we incorporate the Kalb–Ramond field and a constant dilaton into the action. This inclusion introduces the Kalb–Ramond charge density vector and suggests a new method to compute entanglement entropy using the antisymmetric field. In Section 4, we show that bit threads can be exactly reproduced from multiple parallel strings carrying Kalb–Ramond charge, thereby establishing an ex-

plicit correspondence between the string worldsheet and the RT surface. Section 5 explores new results derived from this worldsheet formulation of entanglement entropy: the standard entanglement entropy is obtained from open string charge; through open–closed string duality, the closed string charge yields the Bekenstein–Hawking entropy of the BTZ black hole; the ER=EPR proposal, along with Susskind and Uglum’s conjecture, can be unified within a single framework; and the entanglement entropy, together with the dual RT surface, becomes quantized. Finally, Section 6 is devoted to conclusions and further discussion.

## 2 Motivation

It is important to highlight an approach demonstrating that gravity can emerge from a conformal field theory—namely, string theory. When strings propagate in a curved background, requiring the worldsheet theory to remain conformally invariant after quantization imposes additional dynamical equations on the background metric. These equations serve as the string version of Einstein equations. In the following, we review how gravity emerges from the string worldsheet [39] and explore its connection to entanglement entropy, which motivates our investigation of a new action for the entanglement entropy/RT surface.

Let us recall the Polyakov action for string theory in conformal gauge:

$$S = \frac{1}{4\pi\alpha'} \int d^2\sigma g_{\mu\nu}(X) \partial_\alpha X^\mu \partial^\alpha X^\nu. \quad (14)$$

where  $g_{\mu\nu}(X)$  represents the target-space metric. To determine its dynamics, we first compute the  $\beta$ -function associated with the coupling constant  $g_{\mu\nu}(X)$ . If the  $\beta$ -function vanishes, the quantum version of the Polyakov action remains conformally invariant. To perform this calculation, we introduce Riemann normal coordinates around a spacetime point  $\bar{X}^\mu$ , expanding the coordinates as

$$X^\mu(\tau, \sigma) = \bar{X}^\mu + \sqrt{\alpha'} \mathbb{X}^\mu(\tau, \sigma), \quad (15)$$

where  $\mathbb{X}$  is dimensionless. Under this expansion, the metric takes the form

$$g_{\mu\nu}(X) = g_{\mu\nu}(\bar{X}) - \frac{\alpha'}{3} R_{\mu\lambda\nu\kappa}(\bar{X}) \mathbb{X}^\lambda \mathbb{X}^\kappa + \dots \quad (16)$$

Substituting this into the Polyakov action yields

$$S = \frac{1}{4\pi} \int d^2\sigma \left( g_{\mu\nu} \partial \mathbb{X}^\mu \partial \mathbb{X}^\nu - \frac{\alpha'}{3} R_{\mu\lambda\nu\kappa} \mathbb{X}^\lambda \mathbb{X}^\kappa \partial \mathbb{X}^\mu \partial \mathbb{X}^\nu + \dots \right). \quad (17)$$

This formulation reveals an interacting quantum field theory, where divergences arise from one-loop diagrams. To examine this, we recall the propagator for the scalar field:

$$\langle \mathbb{X}^\lambda(\sigma) \mathbb{X}^\kappa(\sigma') \rangle = -\frac{1}{2} \delta^{\lambda\kappa} \ln |\sigma - \sigma'|^2. \quad (18)$$

At short lengths  $\sigma \rightarrow \sigma'$ , this propagator exhibits a divergence, which can be regularized using dimensional regularization with  $d = 2 + \epsilon$ , leading to

$$\lim_{\sigma \rightarrow \sigma'} \left\langle \mathbb{X}^\lambda(\sigma) \mathbb{X}^\kappa(\sigma') \right\rangle \rightarrow \frac{\delta^{\lambda\kappa}}{\epsilon}. \quad (19)$$

In this limit, the term

$$-\alpha' R_{\mu\lambda\nu\kappa} \mathbb{X}^\lambda \mathbb{X}^\kappa \partial \mathbb{X}^\mu \partial \mathbb{X}^\nu \rightarrow -\frac{\alpha'}{\epsilon} R_{\mu\nu} \partial \mathbb{X}^\mu \partial \mathbb{X}^\nu. \quad (20)$$

This divergence can be canceled by adding the counterterm

$$\frac{\alpha'}{\epsilon} R_{\mu\nu} \partial \mathbb{X}^\mu \partial \mathbb{X}^\nu. \quad (21)$$

which is equivalent to the renormalization

$$\mathbb{X}^\mu \rightarrow \mathbb{X}^\mu + \frac{\alpha'}{\epsilon} R_{\nu}^{\mu} \mathbb{X}^\nu, \quad (22)$$

or, equivalently,

$$g_{\mu\nu} \rightarrow g_{\mu\nu} + \frac{\alpha'}{\epsilon} R_{\mu\nu}, \quad (23)$$

Therefore, the renormalization procedure introduces a UV cutoff, implying that the physical quantities of the theory after quantization generally depend on the energy scale  $\epsilon$ . This dependence breaks conformal symmetry. To preserve conformal symmetry at the quantum level, we must require that the coupling constants—such as the background metric  $G_{\mu\nu}$ —remain independent of  $\epsilon$ . In other words, we demand that the corresponding  $\beta$ -function vanishes:

$$\beta(g) = \alpha' R_{\mu\nu} = 0. \quad (24)$$

which is precisely the vacuum Einstein equation.

On the other hand, let us examine how a similar structure arises in the context of entanglement entropy. To proceed, we introduce Synge's world function  $\Omega$  [27]. The good review of Synge's world function can be found in ref. [28]. Consider a geodesic  $z^\mu(\tau)$  that connects two points in spacetime: the base point  $X'$  and the field point  $X$ . The affine parameter  $\tau$  runs from  $\tau_0$  to  $\tau_1$ , such that:

$$z(\tau_0) := X', \quad z(\tau_1) := X. \quad (25)$$

The tangent vector to the geodesic is  $dz^\mu(\tau)/d\tau$ , as illustrated in figure (3).

Then, Synge's world function  $\Omega(X, X')$  is a scalar function of these two points, defined as:

$$\Omega(X, X') = \frac{1}{2} (\tau_1 - \tau_0) \int_{\tau_0}^{\tau_1} g_{\mu\nu}(z) \frac{dz^\mu}{d\tau} \frac{dz^\nu}{d\tau} d\tau. \quad (26)$$

If we denote the geodesic length between two spacetime points  $X$  and  $X'$  as  $L(X, X')$ , Synge's world function can be rewritten in terms of the geodesic length as

$$\Omega(X, X') = \frac{1}{2} L(X, X')^2. \quad (27)$$

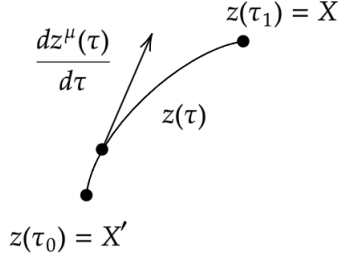


Figure 3: This figure illustrates a geodesic parameterized by  $z(\tau)$ , connecting the base point  $X'$  to the field point  $X$ . The vector  $dz^\mu/d\tau$  represents the tangent vector along the geodesic trajectory.

The partial derivatives of  $\Omega$  with respect to  $X$  and  $X'$  are denoted as  $\Omega_\mu := \partial\Omega/\partial X^\mu$  and  $\Omega_{\mu'} := \partial\Omega/\partial X^{\mu'}$ , respectively. Furthermore, the covariant derivative of  $\Omega_\mu$  with respect to  $X$  is given by  $\Omega_{\mu\nu} := \nabla_\nu \Omega_\mu$ , while its derivative with respect to  $X'$  is  $\Omega_{\mu\nu'} := \partial_{\nu'} \Omega_\mu$ . With these definitions, we introduce an important limit: the coincidence limit, which refers to the limit  $X' \rightarrow X$ , denoted as  $[\dots]$ . Under this limit, the spacetime metric can be expressed as

$$g_{\mu\nu}(X) = -[\Omega_{\mu\nu}] = -\lim_{X' \rightarrow X} \partial_\mu \partial_{\nu'} \Omega(X, X'), \quad g_{\mu\nu}(X) = [\Omega_{\mu\nu}] = \lim_{X' \rightarrow X} \nabla_\nu \partial_\mu \Omega(X, X'). \quad (28)$$

However, taking this limit eliminates valuable information. Remarkably, it is possible to extract spacetime information without imposing the coincidence limit. Instead, we can expand this quantity in the **near-coincidence** regime  $X \rightarrow X'$ :

$$\Omega_{\mu'\nu'}(X, X') = g_{\mu'\nu'}(X') - \frac{1}{3} R_{\mu'\lambda'\nu'\kappa'}(X') \Omega^{\lambda'}(X, X') \Omega^{\kappa'}(X, X') + \dots \quad (29)$$

This expansion closely resembles a procedure in string theory. As previously reviewed, requiring the worldsheet theory to be invariant under conformal transformations leads to the Einstein equations. Here, we pose a similar question: Can we impose conformal symmetry to obtain the Einstein equations? This is a reasonable question, especially since the quantity  $\Omega_{\mu'\nu'}$  is entirely derived from CFT data. If  $\Omega_{\mu'\nu'}$ , encoding geometric information such as the geodesic separation between two spacetime points, emerges from CFT correlators, then requiring conformal invariance at the quantum level may constrain the background geometry. The challenge lies in how to impose conformal symmetry on a known quantity such as the geodesic length. Fortunately, such a possibility exists. The geodesic length in  $\text{AdS}_3$  can be related to the entanglement entropy of a  $\text{CFT}_2$  via the RT formula, which is inherently conformally invariant:

$$S_{\text{vN}}(A : B) = \frac{L(X, X')}{4G_N}. \quad (30)$$

At this step, the  $\text{AdS}_3/\text{CFT}_2$  correspondence enters the story. It is worth noting that this requirement also ensures that the theory remains conformally invariant after quantization. The key point is that

the geodesic length is a classical quantity, while entanglement entropy arises from the quantum theory. The RT formula serves as a bridge between these two regimes, relating a classical geometric object in the bulk to a quantum information-theoretic quantity in the boundary theory. Therefore, maintaining conformal invariance across both sides is essential for the consistency of the correspondence. Based on this argument, if we assume that there exists an action for entanglement entropy expressed in terms of  $\Omega_{\mu'\nu'}(X')$ , we can substitute the entanglement entropy expression (30) into the expansion (29), which leads to the following form of the  $\beta$ -function for the spacetime metric  $g$ :

$$\beta(g) = \ell^2 R_{\mu\nu} = ? \quad (31)$$

However, the precise form of this expression cannot be determined at this stage, as the full action remains unspecified.

In conclusion, whether in string theory or entanglement entropy, the same Einstein equations may be emerged through a similar procedure:

	String theory	Entanglement entropy
1st: Expansion	$g_{\mu\nu} = g_{\mu\nu} - \frac{\alpha'}{3} R_{\mu\lambda\nu\kappa} \mathbb{X}^\lambda \mathbb{X}^\kappa + \dots$	$\Omega_{\mu'\nu'} = g_{\mu'\nu'} - \frac{1}{3} R_{\mu'\lambda'\nu'\kappa'} \Omega^{\lambda'} \Omega^{\kappa'} + \dots$
2nd: Impose symmetry	$\beta(g) = 0$	$L(X, X') = 4G_N S_{\text{vN}}$
3rd: Dynamics for $g_{\mu\nu}$	$R_{\mu\nu} = 0$	$R_{\mu\nu} = ?$

Since, from the perspective of entanglement entropy, we impose conformal symmetry by requiring the geodesic length to correspond to the entanglement entropy—arising from the quantization of the CFT—it is equivalent to selecting the relevant  $\beta$ -function. This suggests that we can replace the RT prescription with a  $\beta$ -function constraint. If this replacement is made, then entanglement entropy effectively becomes a manifestation of string theory, allowing us to formulate its action in direct analogy to the Polyakov action.

In the remainder of this paper, we will demonstrate that the geodesic length—or, equivalently, the symmetric spacetime metric  $g_{\mu\nu}$ —is insufficient to construct a complete and consistent theory. Consequently, it is not possible to derive the full gravitational field equations in the bulk of  $\text{AdS}_3$  using only  $g_{\mu\nu}$ . The resolution, as in string theory, is to introduce the antisymmetric Kalb–Ramond field, which plays a crucial role in ensuring consistency.

### 3 The worldsheet action for entanglement entropy

In this section, we aim to construct an action for the entanglement entropy that fulfills the following criteria:

- The action must be formulated in terms of the entanglement entropy in  $\text{CFT}_2$ , and therefore it should depend explicitly on the coordinates of the  $\text{CFT}_2$ .
- The Einstein equations governing  $\text{AdS}_3$  gravity should be derived from this action.

Before proposing the explicit form of the action, we begin by reviewing recent developments in the study of entanglement entropy for disjoint entangling regions. This will provide crucial insight into how entanglement entropy facilitates the mapping between  $\text{CFT}_2$  coordinates and the corresponding  $\text{AdS}_3$  bulk geometry.

Let us consider two disjoint spacelike intervals,  $A = [x_1, x_2]$  and  $B = [x_3, x_4]$ , separated by the region  $C = [x_2, x_3]$ . By performing a boost, these intervals transform into  $A = [\xi_1, \xi_2] = [(x_1 + it_1), (x_2 + it_2)]$  and  $B = [\xi_3, \xi_4] = [(x_3 + it_3), (x_4 + it_4)]$ , as illustrated in figure (4). The entanglement entropy between regions  $A$  and  $B$  can be computed either through field-theoretic method [40, 41, 42] or via the holographic approach [43, 44]:

$$S_{\text{vN}}(A : B) = \frac{c}{12} \log \left( \frac{1 + \sqrt{\eta}}{1 - \sqrt{\eta}} \right) + \frac{c}{12} \log \left( \frac{1 + \sqrt{\bar{\eta}}}{1 - \sqrt{\bar{\eta}}} \right), \quad (32)$$

where the cross-ratio is defined by

$$\eta = \frac{\xi_{21}\xi_{43}}{\xi_{31}\xi_{42}}, \quad \xi_{ij} \equiv \xi_i - \xi_j, \quad \xi_i = x_i + it_i. \quad (33)$$

Note  $(t_i, x_i)$  are ordinary coordinate of  $\text{CFT}_2$ . We may regroup these coordinates into effective bulk coordinates  $(T, X, Z)$ . The specific regrouping transformation is given in [42, 43, 44], while the general transformation was derived in [14] and reads

$$\begin{aligned} X + iT &= \xi_1 + \frac{|\xi_{13}| |\xi_{14}|}{|\xi_{12}| |\xi_{13}| + |\xi_{34}| |\xi_{24}|} |\xi_{21}|, \\ X' + iT' &= \xi_2 + \frac{|\xi_{23}| |\xi_{24}|}{|\xi_{13}| |\xi_{34}| + |\xi_{12}| |\xi_{24}|} |\xi_{21}|, \\ Z &= \frac{|\xi_{14}| \sqrt{|\xi_{12}| |\xi_{13}| |\xi_{34}| |\xi_{24}|}}{|\xi_{12}| |\xi_{13}| + |\xi_{34}| |\xi_{24}|}, \\ Z' &= \frac{|\xi_{23}| \sqrt{|\xi_{12}| |\xi_{13}| |\xi_{34}| |\xi_{24}|}}{|\xi_{13}| |\xi_{34}| + |\xi_{12}| |\xi_{24}|}. \end{aligned} \quad (34)$$

Then, the cross-ratio becomes

$$\eta = \left| \frac{\xi_{21}\xi_{43}}{\xi_{31}\xi_{42}} \right| = \frac{\Delta Z^2 + \Delta X^2 - \Delta T^2}{(Z + Z')^2 + \Delta X^2 - \Delta T^2}. \quad (35)$$

The entanglement entropy then takes the familiar form:

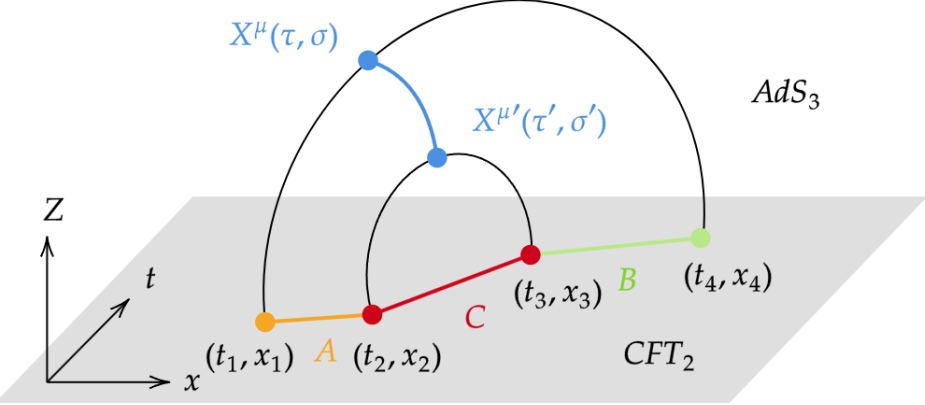


Figure 4: This figure illustrates the blue geodesic in  $AdS_3$ , known as the entanglement wedge cross section (EWCS), whose length is interpreted as the bulk dual of the entanglement entropy between two disconnected entangling regions  $A$  and  $B$ . This result implies that the four boundary coordinates  $(t_i, x_i)$  in the  $CFT_2$  can be conformally mapped to two coordinates  $(\tau_i, \sigma_i)$  in a transformed  $CFT$ , which in turn correspond to two bulk points in  $AdS_3$ .

$$S_{vN}(A : B) = \frac{c}{6} \cosh^{-1} \left( 1 + \frac{\Delta Z^2 + \Delta X^2 - \Delta T^2}{2ZZ'} \right). \quad (36)$$

This result implies that in  $CFT_2$ , the four-points  $(t_1, x_1)$ ,  $(t_2, x_2)$ ,  $(t_3, x_3)$ , and  $(t_4, x_4)$  can be effectively regrouped into two new points,

$$(\tau(t_i, x_i), \sigma(t_i, x_i)), \quad \text{and} \quad (\tau'(t_i, x_i), \sigma'(t_i, x_i)), \quad i = 1, \dots, 4. \quad (37)$$

Through the  $AdS_3/CFT_2$  correspondence—specifically the RT formula—**these  $CFT_2$  coordinates  $(\tau, \sigma)$  can be mapped to the spacetime coordinates  $X^\mu$  of  $AdS_3$  bulk**, corresponding to the two boundary points of the geodesic as illustrated in figure (5). These boundary points in the bulk are then parameterized by

$$X^\mu(\tau, \sigma) \quad \text{and} \quad X^{\mu'}(\tau', \sigma'), \quad (38)$$

where  $\mu = 0, 1, 2$ . Beyond the example discussed here, a well-known instance of this correspondence arises in the study of conformal blocks involving internal twist operators in  $CFT_2$  [46, 47, 48]. In such cases, the two bulk points—interpreted as endpoints of a bulk-to-bulk propagator in  $AdS_3$ —emerge naturally from the global four-point conformal blocks of the boundary theory.

This observation bears a close resemblance to the string worldsheet, where the  $CFT_2$  is embedded into the target space  $X^\mu$ . The key difference, however, is that when computing entanglement entropy for two entangling regions, the coordinates  $(\tau, \sigma)$  and  $(\tau', \sigma')$  are fixed. Consequently, the dual spacetime points  $X^\mu$  and  $X^{\mu'}$  in  $AdS$  are uniquely determined. This means that the geodesic connecting these

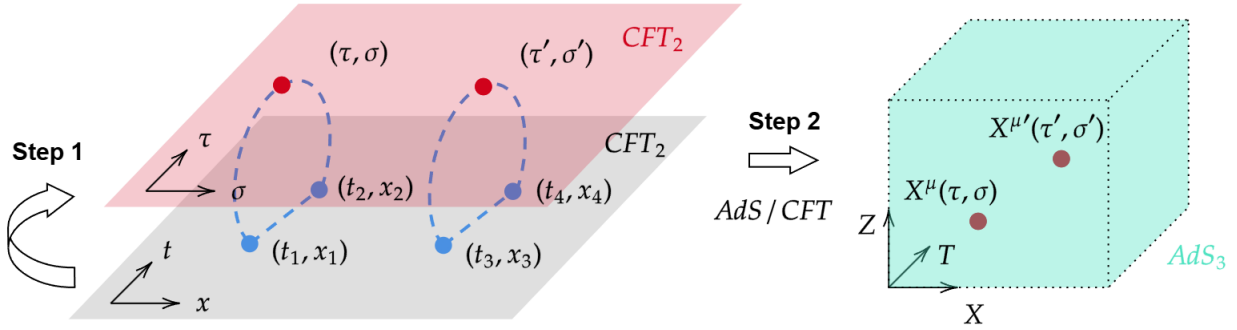


Figure 5: **Step 1:** The coordinates of four points  $(t_i, x_i)$  in  $CFT_2$  can be reorganized into two effective points  $(\tau_i, \sigma_i)$  through a conformal transformation. **Step 2:** These two points  $(\tau_i, \sigma_i)$  are then related to bulk coordinates in  $AdS_3$  via the  $AdS_3/CFT_2$  correspondence.

two points can be described using only a single affine parameter, rather than requiring a full two-dimensional worldsheet description. In this sense, it is not a genuine worldsheet. This is consistent with the general understanding that a geodesic is a fixed geometric feature of the background, unlike a string that propagates dynamically in spacetime.

The situation changes if the entangling regions are varied in time. In this case, both the entanglement entropy and its dual geodesic length evolve accordingly. As a result, the geodesic effectively sweeps through  $AdS_3$ , as illustrated in figure (6). The evolving trajectory generates a two-dimensional surface that can be described by an embedding function  $X^\mu(\tau, \sigma)$ . In other words, By promoting the two bulk endpoints  $X^\mu$  and  $X^{\mu'}$  to fields  $X^\mu(\tau, \sigma)$ ,  $X^{\mu'}(\tau', \sigma')$  we obtain a two-parameter family of geodesics. The union (envelope) of this family defines an emergent two-dimensional surface in the bulk. Motivated by the analogy with string theory, one can then construct an action for this surface—analogous to the Polyakov action—that captures the dynamics of entanglement entropy as the entangling regions change.

Based on these considerations, we now derive key insights for constructing the action, drawing inspiration from how actions are formulated in string theory:

1. Integrating the minimal area  $\int dA$ .
2. Introducing prefactors such as  $\ell^2$  to ensure the action is dimensionless.
3. Parameterizing the action with appropriate variables, e.g.,  $(\tau, \sigma)$  for strings.
4. Building the action entirely from quantities associated with entanglement entropy.

In our setup, a natural area term arises:

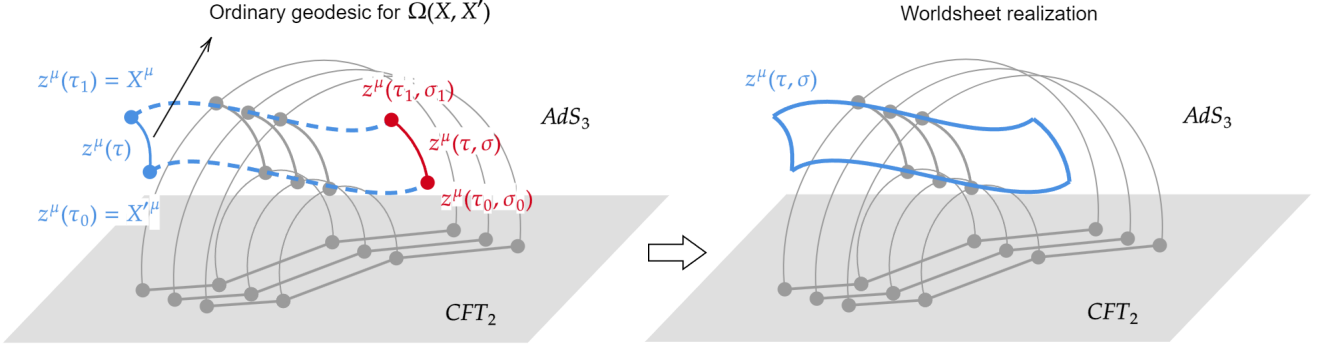


Figure 6: This figure illustrates how a geodesic effectively sweeps out a two-dimensional surface in  $AdS_3$ . In the traditional holographic prescription, the entanglement entropy of  $CFT_2$  is dual to the geodesic length in  $AdS_3$ , with the geodesic endpoints anchored at the boundaries of the chosen entangling region in the  $CFT$ . As the entangling region is deformed—through translation, rotation, stretching, or shrinking—the corresponding bulk geodesic is continuously deformed as well. Collectively, this family of geodesics sweeps out a two-dimensional surface in the bulk, which is naturally analogous to a string worldsheet.

$$2\Omega = g_{\mu\nu}(X) \Omega^\mu \Omega^\nu = \Omega_{\mu\nu} \Omega^\mu \Omega^\nu, \quad (39)$$

which is determined by the entanglement entropy (32) of  $CFT_2$ . By introducing two parameters  $(\tau, \sigma)$ , the single worldline can be promoted to a two-dimensional extended object (worldsheet). This does not require redefining  $\Omega$ ; instead, the derivatives of  $\Omega$  with respect to the two coordinates can be reinterpreted as spanning tangent directions on the effective worldsheet. This structure suggests an action closely analogous to that of the string worldsheet:

$$S_E = \frac{1}{\ell^2} \int d^2\sigma' \Omega_{\mu'\nu'}(X, X') \partial_{\alpha'} \Omega^{\mu'}(X, X') \partial^{\alpha'} \Omega^{\nu'}(X, X'), \quad (40)$$

where  $\partial_{\alpha'} = (\partial_{\tau'}, \partial_{\sigma'})$  acts only on the base point  $X'(\tau', \sigma')$ . Both  $X$  and  $X'$  are boundary-determined bulk points fixed by the entangling regions in the  $CFT$ . Since the two endpoints  $X$  and  $X'$  of any geodesic are interchangeable, there exists a corresponding set of derivatives  $\partial_\alpha = (\partial_\tau, \partial_\sigma)$  acting on the field point  $X(\tau, \sigma)$ . As a result, we obtain a non-local action constructed from the entanglement entropy, which can describe the physics at either of the spacetime coordinates  $X$  or  $X'$ . To verify the consistency of this action, one must check whether it reproduces the entanglement entropy or geodesic length. Before this verification, however, let us examine its physical meaning. Here, instead of treating  $X^\mu(\tau, \sigma)$  as the embedding of a true string, the embedding here is constructed out of geodesics in  $AdS$  that are dual to entangling intervals in the  $CFT_2$ . The Synge's world function  $\Omega(X, X')$  (half the squared geodesic distance) replaces the role of  $X^\mu$  as the basic dynamical variable. Consequently, the action is built directly from entanglement entropy data (through  $\Omega$ ) rather than fundamental fields. The coordinates  $(\tau, \sigma)$  parametrize the varying entangling regions. As these regions evolve, their dual

geodesics sweep out a two-dimensional surface in AdS. This surface is not a fundamental string worldsheet but an effective entanglement worldsheet: a bookkeeping device that tracks the dynamics of entanglement entropy. The action (40) therefore encodes the dynamics of geodesic lengths (equivalently entanglement entropies) as the entangling regions change. The quadratic form in derivatives of  $\Omega^{\mu'}$  resembles the Polyakov action, ensuring that the dynamics is governed by variations of geodesic distance.

To gain intuition, we localize the action to a single spacetime point by introducing a suitable parametrization and expanding around the **near-coincidence limit**  $X \rightarrow X'$ <sup>2</sup>:

$$\Omega_{\mu'\nu'}(X, X') = g_{\mu'\nu'}(X') - \frac{1}{3}R_{\mu'\lambda'\nu'\kappa'}(X')\Omega^{\lambda'}(X, X')\Omega^{\kappa'}(X, X') + \dots \quad (41)$$

Substituting this expansion, the action (40) becomes

$$S_E = \frac{1}{\ell^2} \int d^2\sigma' \left( g_{\mu'\nu'} \partial_{\alpha'} \Omega^{\mu'} \partial^{\alpha'} \Omega^{\nu'} - \frac{1}{3} R_{\mu'\lambda'\nu'\kappa'} \Omega^{\lambda'} \Omega^{\kappa'} \partial_{\alpha'} \Omega^{\mu'} \partial^{\alpha'} \Omega^{\nu'} + \dots \right), \quad (42)$$

where  $\ell$  can be interpreted as the minimal length scale in the expansion. Next, we introduce a tetrad  $e_a^{\mu'}(X')$  at a fixed base point  $X'$ , allowing a neighboring point to be parameterized as

$$\ell \mathbb{X}^a = -e_{\mu'}^a(X') \Omega^{\mu'}(X, X'), \quad (43)$$

where the dual tetrad is defined as  $e_{\mu'}^a = \eta^{ab} g_{\mu'\nu'} e_b^{\nu'}$  and  $\mathbb{X}$  is dimensionless. These coordinates  $\mathbb{X}^a$  correspond to the Riemann normal coordinates (RNC). In this framework, the identity for  $\Omega$  can be rewritten as

$$2\Omega(X, X') = g_{\mu'\nu'} \Omega^{\mu'} \Omega^{\nu'} = g_{ab} e_{\mu'}^a e_{\nu'}^b \Omega^{\mu'} \Omega^{\nu'} = \ell^2 g_{ab} \mathbb{X}^a \mathbb{X}^b, \quad (44)$$

where  $g_{ab} \mathbb{X}^a \mathbb{X}^b$  denotes the squared geodesic distance between the base point  $X'$  and the field point  $X$ . A key feature of RNC is that they shift the base point  $X'$  to the origin, so that  $\mathbb{X}^a = 0$ . On the other hand, since the Synge's world function  $\Omega(X, X')$  depends on both the base point  $X'$  and the field point  $X$ , and since these points can be parameterized by the boundary CFT<sub>2</sub> coordinate  $(\tau, \sigma; \tau', \sigma')$ , we can write  $\Omega(X, X') = \Omega(X(\tau, \sigma), X'(\tau', \sigma'))$ . Consequently, the RNC coordinates  $\mathbb{X}^a$  can also be expressed in terms of the CFT<sub>2</sub> coordinate  $(\tau, \sigma; \tau', \sigma')$  as

$$\ell \mathbb{X}^a(\tau, \sigma; \tau', \sigma') = -e_{\mu'}^a(X'(\tau', \sigma')) \Omega^{\mu'}(X(\tau, \sigma), X'(\tau', \sigma')), \quad (45)$$

In other words, in RNC, we have

$$2\Omega(X, X') = \ell^2 g_{ab} \mathbb{X}^a(\tau, \sigma; \tau', \sigma') \mathbb{X}^b(\tau, \sigma; \tau', \sigma'). \quad (46)$$

---

<sup>2</sup>Note that we may also perform the expansion in the opposite limit  $X' \rightarrow X$ , as given in (29). In this case, the action is modified to

$$S_E = \frac{1}{\ell^2} \int d^2\sigma \Omega_{\mu\nu}(X, X') \partial_{\alpha} \Omega^{\mu}(X, X') \partial^{\alpha} \Omega^{\nu}(X, X').$$

This action is equivalent to (40), since the two endpoints are interchangeable.

Based on these results, the near-coincidence limit of the action (42) can be rewritten in the RNC by using (43), which takes the form

$$S_E = \int d^2\sigma' \left( g_{ab} \partial_{\alpha'} \mathbb{X}^a \partial^{\alpha'} \mathbb{X}^b - \frac{\ell^2}{3} R_{acbd} \mathbb{X}^c \mathbb{X}^d \partial_{\alpha'} \mathbb{X}^a \partial^{\alpha'} \mathbb{X}^b + \dots \right), \quad (47)$$

where  $R_{acbd} := R_{\alpha'\gamma'\beta'\delta'} e_a^{\alpha'} e_c^{\gamma'} e_b^{\beta'} e_d^{\delta'}$ . At the beginning of our construction, the two arguments of Synge's world function were kept distinct,  $X = X(\tau, \sigma)$  and  $X' = X'(\tau', \sigma')$ . because the primed coordinates  $(\tau', \sigma')$  serve as the integration variables in the action. In the near-coincidence limit and in RNC, we identify the two worldsheet points,  $(\tau, \sigma) = (\tau', \sigma')$ . After this identification, the primed coordinates no longer carry any dynamical meaning and become dummy integration variables. They can therefore be relabeled without affecting the integral. Following standard practice in bitensor expansions, we rename  $(\tau', \sigma')$  as  $(\tau, \sigma)$  and drop all primes on tensors and derivatives. This procedure does not lose any information; it simply reflects that the coincidence-limit expansion is performed about a single worldsheet point. We thus obtain the final form of the near-coincidence action,

$$S_E = \int d^2\sigma \left( g_{ab} \partial_\alpha \mathbb{X}^a \partial^\alpha \mathbb{X}^b - \frac{\ell^2}{3} R_{acbd} \mathbb{X}^c \mathbb{X}^d \partial_\alpha \mathbb{X}^a \partial^\alpha \mathbb{X}^b + \dots \right), \quad (48)$$

This coincides with the form of the Polyakov action in a curved background (17) if we identify  $\ell = \sqrt{\alpha'}$ . Therefore, in the near-coincidence limit, the expansion yields a local quadratic action reminiscent of the Polyakov kinetic term for the small separation field  $\hat{X}^a$ . Thus, locally the effective dynamics of geodesic fluctuations is identical to a string worldsheet theory (with curvature corrections given by higher terms in the expansion). A subtle question arises: does the geodesic itself belong to the string worldsheet, given that the action takes a worldsheet-like form? The answer is nuanced. Although the geodesic evolves like a worldsheet, the geodesic itself is not literally a string but sweeps out an effective worldsheet when followed over time. This suggests the geodesic may be interpreted as analogous to a D1-brane trajectory (an 'entangling brane'), with open strings attached to it. In this interpretation, the action effectively describes the dynamics of this brane-like object, rather than a fundamental string. We stress that this identification is conjectural: it is not derived from conventional string theory, but rather suggested by the structural similarities between geodesic dynamics, entanglement entropy, and string worldsheet theory. In this view, the action describes the dynamics of this effective brane, rather than a fundamental string. This reinterpretation not only clarifies the geometric picture but also provides a more precise route for deriving entanglement entropy—or equivalently, the geodesic equation—from the action.

To understand this D-brane configuration, we attempt to reproduce the geodesic equation from the action (40). We begin by varying the action with respect to the base point  $X^{\rho'}$ , such that  $X^{\rho'} \rightarrow X^{\rho'} + \delta X^{\rho'}$ , while keeping  $X'$  fixed. The variation of  $\Omega_{\mu'\nu'}$  yields  $\delta\Omega_{\mu'\nu'} = \partial_{\rho'}\Omega_{\mu'\nu'}\delta X^{\rho'}$ , and that of  $\partial_{\alpha'}\Omega^{\mu'}$  gives  $\delta\Omega_{\mu'\nu'} = \partial_{\rho'}\Omega_{\mu'\nu'}\delta X^{\rho'}$ . Substituting these variations, the action becomes

$$\delta S_E = \frac{1}{\ell^2} \int d^2\sigma' \left[ \partial_{\rho'}\Omega_{\mu'\nu'} \partial_{\alpha'}\Omega^{\mu'} \partial^{\alpha'}\Omega^{\nu'} - 2\partial_{\alpha'} \left( \Omega_{\mu'\nu'} \partial^{\alpha'}\Omega^{\nu'} \right) \partial_{\rho'}\Omega^{\mu'} \right] \delta X^{\rho'}$$

$$+ \frac{1}{\ell^2} \int_{\partial\Sigma} d\tau' \left[ 2n_{\alpha'} \Omega_{\mu'\nu'} \partial_{\rho'} \Omega^{\mu'} \partial^{\alpha'} \Omega^{\nu'} \delta X^{\rho'} \right]_{\sigma=\text{bdy}}, \quad (49)$$

where  $n_\alpha$  is normal to the boundary  $\partial\Sigma$ . Requiring the action to be stationary under arbitrary  $\delta X^\rho$  yields the EOM and boundary condition:

$$\begin{aligned} \text{EOM : } & \partial_{\rho'} \Omega_{\mu'\nu'} \partial_{\alpha'} \Omega^{\mu'} \partial^{\alpha'} \Omega^{\nu'} - 2\partial_{\alpha'} \left( \Omega_{\mu'\nu'} \partial^{\alpha'} \Omega^{\nu'} \right) \partial_{\rho'} \Omega^{\mu'} = 0, \\ \text{B.C. : } & n_{\alpha'} \Omega_{\mu'\nu'} \partial_{\rho'} \Omega^{\mu'} \partial^{\alpha'} \Omega^{\nu'} \delta X^{\rho'} \Big|_{\partial\Sigma} = 0, \end{aligned} \quad (50)$$

In the coincidence limit, these reduce to

$$[\Omega_{\mu'\nu'}] = g_{\mu\nu}, \quad [\Omega_{\mu'}] = 0, \quad [\partial_{\alpha'} \Omega^{\mu'}] = \partial_\alpha X^\mu, \quad (51)$$

which leads to the standard string-theoretic form:

$$\begin{aligned} \text{EOM : } & \partial_\alpha \partial^\alpha X^\lambda + \Gamma_{\mu\nu}^\lambda \partial_\alpha X^\mu \partial^\alpha X^\nu = 0, \\ \text{B.C. : } & g_{\mu\nu} n_\alpha \partial^\alpha X^\mu \delta X^\nu \Big|_{\partial\Sigma} = 0. \end{aligned} \quad (52)$$

To obtain the endpoint geodesic equation, we fix the static gauge so that the boundary is parameterized by  $\tau$ . We then decompose the indices  $\mu$  into tangent directions  $a$  (along the D-brane/RT surface) and normal directions  $i$  (transverse), or vice versa. For the normal directions we impose Dirichlet boundary conditions,  $\delta X^i \Big|_{\partial\Sigma} = 0$ , while for the tangential directions we impose Neumann boundary conditions,  $g_{\mu\nu} n_\alpha \partial^\alpha X^a \Big|_{\partial\Sigma} = 0$ . Applying these conditions, the EOM at the boundary becomes

$$\ddot{X}^a + \Gamma_{bc}^a \dot{X}^b \dot{X}^c = 0. \quad (53)$$

which is precisely the geodesic equation for the endpoints along the D-brane. This result can be interpreted as shown in figure (7). In our setup, the spacetime point  $X$ , representing a geodesic endpoint, is parameterized by two-dimensional coordinates  $(\tau, \sigma)$ . Consequently, the geodesic sweeps out a two-dimensional surface whose dynamics are governed by the non-local EOM and boundary conditions (50). Taking the near-coincidence limit  $X \rightarrow X'$  reduces these to the local EOM and boundary conditions (52), in full agreement with string theory. Under the appropriate boundary conditions, the boundary  $\partial\Sigma$  obeys the geodesic EOM (53). Thus, the proposed action (40) indeed contains the expected geodesic dynamics.

Nevertheless, this geodesic equation is general and applies to arbitrary geodesics. At this stage, we cannot restrict the geodesics to reside exclusively in  $\text{AdS}_3$ . Moreover, it remains unclear how the gravitational field equations for the  $\text{AdS}_3$  gravity emerge from this action. These issues contradict our initial premise that  $\Omega$ , and hence the action, originates from entanglement entropy in the  $\text{AdS}_3/\text{CFT}_2$  framework. In other words, the action constructed thus far is incomplete.

To obtain the complete action, let us recall how Einstein equations emerge from string worldsheet theory. Since our proposed action reduces to the Polyakov action in the near-coincidence limit, the

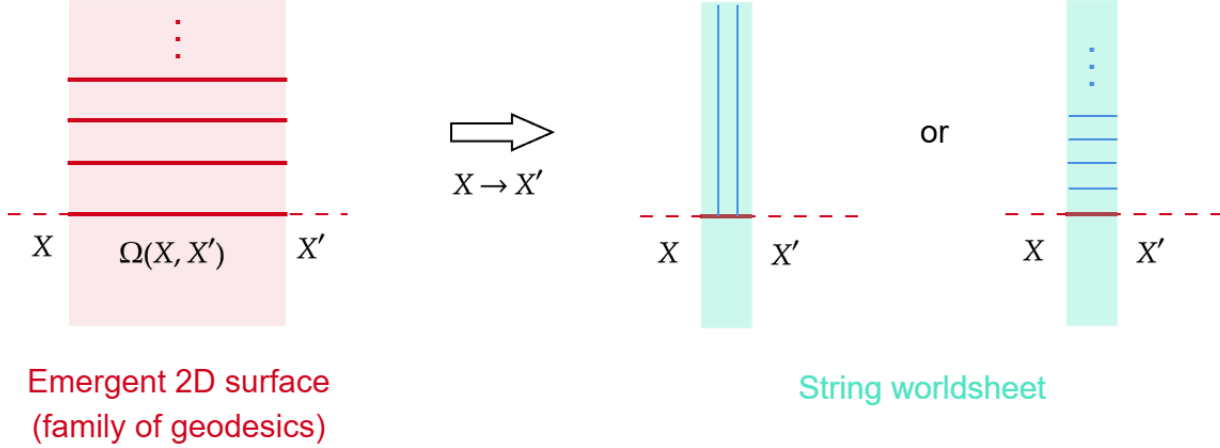


Figure 7: The left panel shows how a family of geodesics between  $X$  and  $X'$  (red lines) sweeps out an effective two-dimensional surface. The length of each geodesic corresponds to the bulk dual of a CFT entanglement entropy. In the near-coincidence limit  $X \rightarrow X'$ , this surface acquires the structure of a string worldsheet, with the Polyakov action emerging naturally. The right panel illustrates this worldsheet. Depending on the gauge choice, the open string (blue lines) can fluctuate along horizontal or vertical directions, while its endpoints obey the geodesic equation for a point-like particle.

same logic applies here. In conventional string theory, preservation of conformal symmetry at the quantum level requires the vanishing of the  $\beta$ -function for  $g_{ab}$ . For instance, when the Polyakov action includes only the spacetime metric, the corresponding  $\beta$ -function is

$$\beta(g) = \ell^2 R_{ab}. \quad (54)$$

In our case, if we demand that  $\Omega$  corresponds to the squared geodesic length in the bulk of  $\text{AdS}_3$ , then the metric  $g_{ab}$  must be the  $\text{AdS}_3$  metric. Substituting this into the  $\beta$ -function gives

$$\beta(g) = \ell^2 R_{ab} = -2 \frac{\ell^2}{l_{\text{AdS}}^2} g_{ab} \neq 0. \quad (55)$$

This  $\beta$ -function is manifestly non-vanishing, which implies that it is impossible to derive the gravitational field equations of  $\text{AdS}_3$  only from the RT surface and its corresponding  $\Omega$ . To achieve a vanishing  $\beta$ -function when evaluated on the  $\text{AdS}_3$  background, the only resolution is to include an antisymmetric field from the outset. This leads us to modify the action as follows:

$$S_E = \frac{1}{\ell^2} \int d^2 \sigma' \sqrt{\gamma} \left( \gamma^{\alpha' \beta'} \Omega_{\mu' \nu'}(X, X') + i \epsilon^{\alpha' \beta'} \mathcal{B}_{\mu' \nu'}(X, X') \right) \partial_{\alpha'} \Omega^{\mu'}(X, X') \partial_{\beta'} \Omega^{\nu'}(X, X'). \quad (56)$$

where  $\mathcal{B}_{\mu' \nu'}(X, X')$  becomes

$$\begin{aligned} \mathcal{B}_{\mu'\nu'}(X') &= B_{\mu'\nu'}(X') + \nabla_{\lambda'} B_{\mu'\nu'} \Omega^{\lambda'}(X, X') + \frac{1}{2} \left( \nabla_{\alpha'} \nabla_{\beta'} B_{\mu'\nu'}(X') - \frac{1}{3} R_{\alpha'\mu'\beta'}^{\lambda'} B_{\lambda'\nu'} \right. \\ &\quad \left. - \frac{1}{3} R_{\alpha'\nu'\beta'}^{\lambda'} B_{\lambda'\mu'} \right) \Omega^{\alpha'}(X, X') \Omega^{\beta'}(X, X') + \dots, \end{aligned} \quad (57)$$

in the **near-coincidence limit**. Moreover, in addition to the inclusion of the Kalb–Ramond field, it is also necessary to incorporate the dilaton field  $\phi$  and the cosmological constant term  $4/k$ , as is standard in non-critical string theory. The role of the dilaton will be explained in Section 4. All massless sectors of the closed string thus become indispensable in establishing the correspondence between the string worldsheet theory and entanglement entropy. Employing RNC and using the relation  $B_{ab} := B_{\alpha'\beta'} e_a^{\alpha'} e_b^{\beta'}$ , the vanishing of the  $\beta$ -functions for  $g_{ab}$ ,  $B_{ab}$  and  $\phi$  leads to the following gravitational field equations:

$$\begin{aligned} R_{ab} + 2\nabla_a \nabla_b \phi - \frac{1}{4} H_{acd} H_b^{cd} &= 0, \\ \nabla^a \left( e^{-2\phi} H_{abc} \right) &= 0, \\ 4\nabla^2 \phi - 4(\nabla \phi)^2 + R - \frac{1}{12} H^2 + \frac{4}{k} &= 0. \end{aligned} \quad (58)$$

This system now admits a solution that is fully consistent with our entanglement entropy setup, with  $g_{ab}$  given by the  $\text{AdS}_3$  metric, the Kalb–Ramond field strength  $H_{abc} = \frac{2}{l_{AdS}^2} \epsilon_{abc}$ , a constant dilaton  $\phi$  and  $k = l_{AdS}^2$  [49]. Under this solution, the connection  $\Gamma_{bc}^a$  introduced in equation (53) is modified to include the contribution from the Kalb–Ramond field:  $\Gamma_{bc}^a = \Gamma_{bc}^a - \frac{1}{2} H_{bc}^a$ . With this modification, the geodesic equation reproduces the motion of a point-like particle in  $\text{AdS}_3$ .

In summary, we argue that our proposed action provides a valid description of the  $\text{CFT}_2$  entanglement entropy for the following reasons:

1. The action is fully constructed from the entanglement entropy itself,  $\Omega(X, X') \sim S_{\text{vN}}(A : B)^2$ .
2. The equations of motion and boundary conditions derived from this action naturally include the geodesic equation in  $\text{AdS}_3$ .
3. By imposing conformal symmetry, the action yields the Einstein equations of  $\text{AdS}_3$  gravity in the near-coincidence limit.

Moreover,

- This result suggests a framework for understanding the relation between Klein–Gordon equation + renormalization group (RG) equations and general relativity (GR). At the level of the effective worldsheet theory, the dynamics are governed by a QFT whose equations of motion reduce to the two-dimensional Klein–Gordon equation for bosonic fields. Expanding around the near-coincidence limit and employing RNC introduces interaction terms associated with background fields, which in turn manifest as RG equations. The requirement of conformal symmetry then enforces the emergence of the Einstein equations in  $\text{AdS}_3$ .

Finally, it is worth recalling previous developments of string theory on  $\text{AdS}_3$  in the context of the AdS/CFT correspondence. The subject originates from the duality between type IIB superstring theory on  $\text{AdS}_3 \times S^3 \times T^4$  and a CFT in the moduli space of the symmetric orbifold of  $T^4$  [50, 51]. This duality was subsequently refined to identify the tensionless limit of strings with minimal pure NS-NS flux with the symmetric orbifold  $\text{Sym}^N(T^4)$  [52, 53, 54], and later extended beyond the tensionless regime through deformations by exactly marginal operators [55, 56, 57, 58, 59]. On the worldsheet, strings in  $\text{AdS}_3$  are described by the  $SL(2, \mathbb{R})$  WZW model [60, 61, 62], where the inclusion of spectrally flowed representations of the affine algebra is essential to account for the physics of long strings [63, 64, 65].

In this work, however, our focus is not on the quantization of strings in  $\text{AdS}_3$  or on the construction of their precise CFT duals. Instead, our analysis originates entirely from the study of entanglement entropy, from which a Polyakov-like action emerges locally as a consequence of the underlying entanglement dynamics, as discussed above.

In the following sections, we will present further evidence demonstrating that this new action and framework provide novel methods and lead to new results for the study of entanglement entropy.

## 4 Kalb–Ramond charge density as bit threads

If our derivation of the worldsheet action for entanglement entropy is correct, there must exist an additional, previously unrecognized antisymmetric field in the entanglement theory, which leads to the consistent gravitational field equations for the  $\text{AdS}_3$ . Just as the RT surface gives rise to a symmetric field—the spacetime metric  $g_{ab}$ —there should exist a bulk quantity on equal footing that sources an antisymmetric field  $B_{ab}$ :

$$g_{ab} \iff B_{ab}. \quad (59)$$

To identify this quantity, let us recall the physical meaning of the Kalb–Ramond field  $B_{ab}$ . In string theory, the worldsheet term  $B_{ab}\partial_\alpha X^a\partial_\beta X^b$  describes the coupling of the string to the antisymmetric Kalb–Ramond field. This is the natural generalization of the electric coupling between a point-like particle and the electromagnetic field. In this sense, the string carries an electric Kalb–Ramond charge. To see this, recall the definition of electric current in electromagnetism:

$$\frac{\partial F^{ab}}{\partial x^b} = j^a, \quad (60)$$

where  $j^0$  denotes the electric charge density. Analogously, the field strength  $H^{abc}$  of the Kalb–Ramond field satisfies:

$$\frac{\partial H^{abc}}{\partial x^c} = \kappa^2 j^{ab}, \quad (61)$$

The Kalb–Ramond charge density vector is given by  $\vec{j}^0 \equiv j^{0a}$ . This vector possesses two important properties that guide us in identifying its entanglement entropy analogue:

1. The charge density vector is tangent to the string.
2. The string charge density is a divergenceless vector  $\nabla \cdot \vec{j}^0 = 0$ .

In the context of entanglement entropy, there exists a closely analogous quantity: a divergenceless vector field defined on the RT surface, encoding information about entanglement—namely, the bit threads [33]. These are flow lines in AdS spacetime that begin and end on the boundary and thread through the bulk, providing a dual description of entanglement entropy. Previous studies exploring the connection between bit threads and Einstein's equations can be found in [66, 67]. For example, consider the flux through region  $A$  which is defined as

$$\int_A v \equiv \int_A \sqrt{h} n_\mu v^\mu = \int_{\gamma_A} v, \quad (62)$$

where  $h$  is the induced metric on  $A$ , and  $n_\mu$  is the unit normal to  $A$ . The equality follows from the fact that  $A$  and  $\gamma_A$  are homologous; thus, the net flux entering the bulk volume between them must vanish. Moreover, the flux is bounded by the area of the RT surface:

$$\int_A v = \int_{\gamma_A} v \leq C \text{area}(\gamma_A). \quad (63)$$

The entanglement entropy is given by

$$S_{\text{vN}} = \frac{\text{area}(\gamma_A)}{4G_N} = \max_v \int_A v, \quad (64)$$

with  $C = 1/4G_N^{(3)}$ . In short, in an oriented and bounded Riemannian manifold with a positive constant  $C = 1/4G_N^{(3)}$ , the bit thread configuration is described by a divergenceless, bounded vector field  $v$ . This vector field  $v$ , referred to as a flow, satisfies the following conditions:

1. The field  $v$  is perpendicular to the RT surface. If  $v(A)$  denotes the set of flow lines sourced from a boundary region  $A$ , then its flux equals the area of the RT surface  $\gamma_A$  homologous to  $A$ .
2. The field is divergenceless and bounded:  $\nabla \cdot v = 0$ ,  $|v| \leq 1/4G_N^{(3)}$ .

Therefore, it is straightforward to verify the equivalence between  $\vec{j}^0$  and  $v$ , as both vector fields are defined on the same time slice of  $\text{AdS}_3$  and obey identical divergenceless conditions:  $\nabla \cdot \vec{j}^0 = 0$  and  $\nabla \cdot v = 0$ . If these two vectors coincide, it provides a natural identification between the worldsheet theory and entanglement entropy: one may relate the string charge density vector  $\vec{j}^0$  to the bit thread vector field  $v$ . On the other hand, in this configuration, the Kalb–Ramond charge density vector  $\vec{j}^0$  lies along the string in the direction of increasing  $\sigma$ , reflecting the string's orientation. Moreover, it is important to note that the reparameterization invariance of the string worldsheet is broken in the presence of the Kalb–Ramond field. The reason is that the corresponding term  $B_{ab}\partial_\alpha X^a \partial_\beta X^b$  in the worldsheet action changes sign under a reversal of the worldsheet coordinates  $(\tau, \sigma)$ . As a result, strings become oriented when the Kalb–Ramond field is included, and the charge density vector  $\vec{j}^0$  is aligned

with the  $\sigma$ -direction, rather than the  $\tau$ -direction. This orientation plays a crucial role in identifying the dual of the charge density vector in the entanglement entropy picture.

On the other hand, beyond establishing the relation between  $\vec{j}^0$  and  $v$ , identifying the counterpart of the RT surface on the string worldsheet is more subtle. This is because there is no natural prescription to extract geodesics on the worldsheet embedded in  $\text{AdS}_3$ . However, an important object in string theory that has not yet been incorporated into our discussion—the D-brane—offers a consistent resolution. Together with the previously proposed correspondence between  $\vec{j}^0$  and the bit thread vector  $v$ , we identify three guiding constraints that link the worldsheet geometry to the RT surface:

1. The geodesic on the worldsheet must coincide with the RT surface. This is because the function  $\Omega(X, X')$  in the action originates from the entanglement entropy, which is itself determined by the RT surface.
2. Bit threads are orthogonal to the RT surface. Consequently, the string charge density vector  $\vec{j}^0$  (or equivalently, the orientation of open strings) must also be orthogonal to the corresponding geodesic on the worldsheet.
3. The string charge density vector  $\vec{j}^0$  must be divergenceless and cannot terminate at any point in spacetime. This implies that strings must either be closed or extend infinitely; in particular, open strings cannot end on a boundary unless a mechanism exists to maintain current continuity.

These conditions suggest a natural geometric configuration: while it may be difficult to isolate geodesics on the worldsheet, we can instead fix the boundary of the worldsheet to follow the geodesic in  $\text{AdS}$ . In this picture, the boundary of the worldsheet—the D-brane—is identified with the RT surface. Furthermore, to satisfy the divergenceless condition, open strings cannot simply end on the D-brane. A consistent solution is to consider pairs of open strings attached to opposite sides of the D-brane. When the number of open strings reaches a maximal density and all strings are orthogonal to the D-brane, strings from the two sides can smoothly connect across the D-brane, ensuring the continuity of  $\vec{j}^0$  and the absence of any current sink or source.

In the following subsections, we will demonstrate how to approach this set-up and explicitly derive the bit thread vector field  $v$  from the string charge density  $\vec{j}^0$ .

#### 4.1 Set-up

To make this configuration explicit, we consider two sets of stationary, parallel open strings stretched along the  $z_+$ - and  $z_-$ -directions in three-dimensional flat spacetime  $(t_\pm, z_\pm, x_\pm)$ , as illustrated in figure (8). The first set of parallel strings, parameterized by  $(\tau^+, \sigma^+)$ , and the second set, parameterized by  $(\tau^-, \sigma^-)$ , are embedded in two-dimensional target spaces:

$$X_-^t(\tau^-, \sigma^-), X_-^z(\tau^-, \sigma^-), X_-^x(\tau^-, \sigma^-), \quad X_+^t(\tau^+, \sigma^+), X_+^z(\tau^+, \sigma^+), X_+^x(\tau^+, \sigma^+), \quad (65)$$

respectively. We adopt the static gauge by setting

$$X_{\pm}^t(\tau^{\pm}, \sigma^{\pm}) = \tau^{\pm}, \quad X_{\pm}^z(\tau^{\pm}, \sigma^{\pm}) = \sigma^{\pm}, \quad X_{\pm}^x(\tau^{\pm}, \sigma^{\pm}) = x_n^{\pm}, \quad (66)$$

where the constants  $x_n^{\pm}$  specify the endpoints of the strings at the  $n$ -th position along the  $x$ -direction. The separation between two adjacent strings is denoted by  $d_s$ . At the string endpoints, we impose Dirichlet boundary conditions:  $\partial_{\tau^{\pm}} X_{\pm}^z|_{0,b} = 0$ .

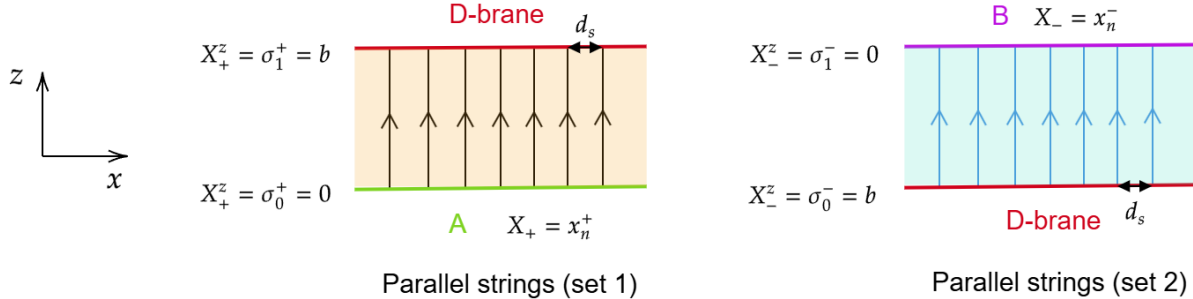


Figure 8: This figure depicts two sets of parallel open strings in static gauge, stretched along the  $z$ -direction with an inter-string separation of  $d_s$ . The green, purple, and red solid lines represent D-branes, with the red D-brane serving as the central focus of this discussion, corresponding to the RT surface. The open string endpoints satisfy Dirichlet boundary conditions in the  $z$ -direction. These two sets of parallel strings can be embedded in a time slice of BTZ black brane and smoothly joined along the red D-brane. Crucially, the strings asymptotically approach the green and purple D-branes at the AdS boundary, ensuring that the string charge density vector remains divergenceless throughout the configuration. In the following discussion, we will map these two sets of parallel strings onto two regions of the Poincaré patch of a time slice of  $\text{AdS}_3$ , as illustrated in figure (9). This mapping will make the underlying physics more transparent.

We now embed the two worldsheets into a time slice of BTZ black brane, equipped with the metric

$$dS_{\pm}^2 = \frac{l_{\text{AdS}}^2}{z_{\pm}^2} \left( -\left(1 - (z_{\pm}/b)^2\right) dt^2 + \frac{dx_{\pm}^2}{1 - (z_{\pm}/b)^2} + dz_{\pm}^2 \right), \quad (67)$$

where  $t_+ = t_- = t$ ,  $x_{\pm} \in \mathbb{R}$  and  $z_{\pm} \in (0, b]$ . In this coordinate system, the planar horizon—which we identify with the RT surface—is located at  $z_{\pm} = b$ . This is the junction of the two strings, and continuity across this junction implies  $x_+ = x_- = x$  along the sewing line. From the boundary conditions, we see that open strings on either side of the D-brane can be smoothly joined. Specifically, at  $z_{\pm} = b$ , the boundary conditions

$$\partial_{\tau} X_{\pm}^z|_b = \partial_{\tau} X_{\mp}^z|_b = 0, \quad \partial_{\sigma^+} X_{\pm}^z|_b = \partial_{\sigma^-} X_{\mp}^z|_b = 0, \quad X_{\pm}^x = X_{\mp}^x = x_n, \quad (68)$$

ensure that both the temporal and spatial derivatives of the string embedding functions match at the junction. To study whether the string charge density vectors  $\vec{j}_{\pm}^0$  from the two open strings can be connected at the D-brane, we recall the general expression for the string current  $j^{\mu\nu}$  for a single string:

$$j^{\mu\nu}(x) = \int d\sigma^2 \delta^D(x - X(\tau, \sigma)) (\partial_\tau X^\mu \partial_\sigma X^\nu - \partial_\tau X^\nu \partial_\sigma X^\mu), \quad (69)$$

This expression is defined at spacetime points  $x$  that lie on the worldsheet. In the static gauge, where  $X^0 = \tau$ , the spatial components simplify to

$$\vec{j}^0(x) = \int d\sigma \delta(\vec{x} - \vec{X}(\tau, \sigma)) \partial_\sigma \vec{X}(\tau, \sigma), \quad (70)$$

where  $\vec{X}(\tau, \sigma) \equiv (X^z(\tau, \sigma), X^x(\tau, \sigma))$  denotes the embedding of the string in the  $(z, x)$ -plane, and  $x$  refers to the spatial components of the target spacetime. Returning to our configuration, we evaluate  $\vec{j}_\pm^0(x)$  for the two strings. Since the setup lies within a time slice of  $\text{AdS}_3$ , the string charge density vectors are maximized along geodesics. As a result, for each spacetime point  $x$  on the D-brane, there exists a unique  $\vec{j}_\pm^0(x)$  vector flowing into or out of the D-brane. Specifically, at every point  $x_n$  on the D-brane, there is a pair of charge density vectors that converge. The continuity conditions previously discussed ensure that the spatial derivatives  $\partial_\sigma \vec{X}$  are matched across the junction. Consequently, the total string charge density vectors can be smoothly connected as

$$\begin{aligned} \vec{j}^0(x) &= \vec{j}_+^0(x_+) \cup \vec{j}_-^0(x_-) \\ &= \int d\sigma^+ \delta(\vec{x} - \vec{X}_+(\tau, \sigma^+)) \partial_{\sigma^+} \vec{X}_+(\tau, \sigma^+) \\ &\quad + \int d\sigma^- \delta(\vec{x} - \vec{X}_-(\tau, \sigma^-)) \partial_{\sigma^-} \vec{X}_-(\tau, \sigma^-) \\ &= \int d\sigma \delta(\vec{x} - \vec{X}(\tau, \sigma)) \partial_\sigma \vec{X}(\tau, \sigma), \end{aligned} \quad (71)$$

ensuring the global divergencelessness of  $\vec{j}^0$  in the full D-brane-included configuration. In other words, the endpoints of two open strings can join to form a new open string. This mechanism has also been used to study open-string dynamics in the closed-string vacuum and to explain how closed strings emerge as weakly coupled excitations [68]. In such a scenario, if open strings are charged under a  $U(1)$  gauge field that becomes confined, the endpoints of an open string are connected by an electric flux tube. The combination of the open string and this flux tube then effectively forms a closed string. Moreover, this result is also consistent with the edge-mode constraints on the two sides of the horizon in the low-energy description, where the number and positions of the string endpoints must match on both sides [11]. These endpoints are effectively frozen on the horizon due to the infinite gravitational time dilation.

To relate this setup to the bit thread picture, we perform the coordinate transformation introduced in [34, 35] and further developed in [36]:

$$y_\pm = \frac{b \sinh(x_\pm/b)}{\cosh(x_\pm/b) \pm \sqrt{1 - (z_\pm/b)^2}}, \quad w_\pm = \frac{z_\pm}{\cosh(x_\pm/b) \pm \sqrt{1 - (z_\pm/b)^2}}. \quad (72)$$

This transforms the BTZ black brane metric (67) into the familiar Poincaré patch of time slice of  $\text{AdS}_3$ :

$$dS_{\pm}^2 = \frac{l_{\text{AdS}}^2}{w_{\pm}^2} (dy_{\pm}^2 + dw_{\pm}^2). \quad (73)$$

Under this map, the D-brane/RT surface is represented by the semicircle  $y_{\pm}^2 + w_{\pm}^2 = b^2$ . Parallel strings (set 1) occupies the interior orange region  $y_{\pm}^2 + w_{\pm}^2 < b^2$ , and Parallel strings (set 2) covers the exterior cyan region  $y_{\pm}^2 + w_{\pm}^2 > b^2$ , as illustrated in figure (9).

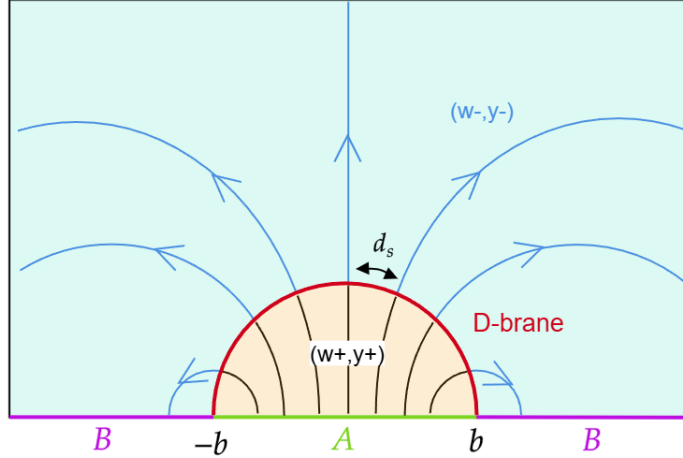


Figure 9: Two open string worldsheets, originally illustrated in figure (8), are mapped into the Poincaré patch of a time slice of  $\text{AdS}_3$ . The green, purple, and red lines denote D-branes, with the red D-brane corresponding to the RT surface. Parallel strings 1 (orange) is described by the region  $y_{\pm}^2 + w_{\pm}^2 < b^2$ , while parallel strings 2 (cyan) occupies the region  $y_{\pm}^2 + w_{\pm}^2 > b^2$ , where  $b$  is the radius of the semicircle. The string charge density vectors from both worldsheets are smoothly connected at the red D-brane, ensuring the combined vector field remains divergenceless.

## 4.2 Deriving bit threads in string theory

Building on the setup from the previous subsection, we now attempt to show that bit threads can be exactly derived from multiple parallel stationary strings carrying Kalb–Ramond charges. To this end, we recall the solutions presented by Dabholkar et al. in the low-energy analysis of macroscopic superstrings [30, 31, 32]. A recent review is provided in [69]. These macroscopic superstrings play a role analogous to solitons in supersymmetric field theories. The relevant low-energy effective action, obtained as the localization of our proposed action (40) and incorporating the macroscopic string as a source term, is given by

$$S = \frac{1}{2\kappa^2} \int d^3x \sqrt{-g} e^{-2\phi} \left( R + 4(\nabla\phi)^2 - \frac{1}{12}H^2 + \frac{4}{k} \right) + S_{\sigma}, \quad (74)$$

with the string source described by the sigma model

$$S_\sigma = -\frac{1}{4\pi\alpha'} \int d^2\sigma \left( \sqrt{\gamma} \gamma^{mn} \partial_m X^a \partial_n X^b g_{ab} + \epsilon^{mn} \partial_m X^a \partial_n X^b B_{ab} \right), \quad (75)$$

This action describes a macroscopic string carrying Kalb–Ramond charge, propagating in the background and interacting with background fields. The equations of motion follow as

$$\begin{aligned} R^{ab} + 2\nabla^a \nabla^b \phi - \frac{1}{4} H^{acd} H_{cd}^b &= \kappa^2 T^{ab}, \\ \nabla_a \left( e^{-2\phi} H^{abc} \right) &= \frac{\kappa^2}{\pi\alpha'} j^{bc} \\ 4\nabla^2 \phi - 4(\nabla\phi)^2 + R - \frac{1}{12} H^2 + \frac{4}{k} &= 0, \end{aligned} \quad (76)$$

with source terms

$$\begin{aligned} T^{ab} &= -\frac{e^{2\phi}}{2\pi\alpha'\sqrt{-g}} \int d^2\sigma \sqrt{\gamma} \gamma^{mn} \partial_m X^a \partial_n X^b \delta^{(3)}(x - X(\tau, \sigma)), \\ j^{ab} &= \frac{1}{\sqrt{-g}} \int d^2\sigma \left( \frac{\partial X^a}{\partial \tau} \frac{\partial X^b}{\partial \sigma} - \frac{\partial X^b}{\partial \tau} \frac{\partial X^a}{\partial \sigma} \right) \delta^{(3)}(x - X(\tau, \sigma)). \end{aligned} \quad (77)$$

Note that we extract a factor of  $1/\alpha'$  from  $j^{ab}$  in (77) and incorporate it into the second equation of motion in (76). This adjustment is necessary because the dimension of  $j^{ab}$  is  $[L]^{-1}$  in the case of two spatial dimensions. The usual solutions of these EOM (76) are known as string solitons [30, 31, 32]. However, in our case, we require the solution to remain  $\text{AdS}_3$ , which in turn demands that the string source does not significantly modify the background geometry.

To approach this solution of the EOM (76), let us first recall that the action originates from entanglement entropy via the  $\text{AdS}_3/\text{CFT}_2$  correspondence. This implies that bulk gravity is weak, i.e.  $\kappa^2 = 8\pi G_N^{(3)} \rightarrow 0$ , while the central charge diverges,  $c \rightarrow \infty$ , in the CFT at the conformal boundary. Parametrically, the three-dimensional Newton constant scales as

$$16\pi G_N^{(D)} = \left( 2\pi\sqrt{\alpha'} \right)^{D-2} g_s^2 (2\pi)^{-1}, \quad (78)$$

so that

$$\frac{\kappa^2}{\pi\alpha'} = \frac{g_s^2}{2\pi\sqrt{\alpha'}}. \quad (79)$$

This factor multiplies the string-source terms in the EOM (76). If the dilaton field is trivial,  $\phi = 0$ , so that  $g_s = 1$ , then in the weak-gravity limit  $\kappa^2 \sim \sqrt{\alpha'} \rightarrow 0$  the prefactor diverges, making it difficult to find consistent  $\text{AdS}_3$  solutions. To suppress the backreaction of  $\mathcal{N}$  string sources on the  $\text{AdS}_3$  background, we therefore require

$$g_s^2 = e^{2\phi_0} \ll \frac{\sqrt{\alpha'}}{l_{\text{AdS}}} \cdot \frac{1}{\mathcal{N}}, \quad (80)$$

where  $l_{\text{AdS}}$  is introduced to render the string coupling dimensionless and  $\phi_0$  is a constant dilaton. Thus, the simplest choice for  $g_s$  is

$$g_s^2 = e^{2\phi_0} = \frac{\sqrt{\alpha'}}{l_{\text{AdS}}} \cdot \frac{\epsilon}{\mathcal{N}}, \quad \epsilon \ll 1. \quad (81)$$

This necessity explains why the dilaton must be incorporated into our proposed action (40).

This scaling for the string coupling is closely analogous to the D1–D5/F1-NS5 system [70, 71, 72]. In type IIB string theory on  $\text{R}^4 \times \text{R}^2 \times \text{T}^4$ , consider  $Q_1$  fundamental strings on  $\text{R}^2$  bound to  $Q_5$  NS5-branes on  $\text{R}^2 \times \text{T}^4$ . In the near-horizon limit the geometry becomes  $\text{AdS}_3 \times \text{S}^3 \times \text{T}^4$ . There the string coupling is [62]

$$g_s^2 = \frac{1}{Q_1 \sqrt{Q_5}}, \quad l_{\text{AdS}} = \sqrt{Q_5} \sqrt{\alpha'}, \quad (82)$$

which can be rewritten as

$$g_s^2 = \frac{\sqrt{\alpha'}}{l_{\text{AdS}}} \cdot \frac{1}{Q_1}, \quad (83)$$

where the central charge of the dual CFT<sub>2</sub> is  $c = 6Q_1Q_5 \gg 1$ . Since  $\mathcal{N}$  of (81) also relates to the charge of fundamental string (to be examined later), this agrees with our condition above, showing that the same type of scaling naturally appears in a well-understood brane system. Moreover, it is also shown that when  $Q_1, Q_5 \gg 1$ , the long string does not significantly affect the background geometry in this system [51].

Now, let us return to our setup. We begin by solving the EOM (76) in the limit  $\frac{\kappa^2}{\pi\alpha'} \rightarrow 0$ . In this limit, we consider only the leading-order solution. The higher-order corrections to the spacetime can then be interpreted as quantum corrections, which complete the generalized entropy prescription [73, 74]. In this regime, the solution is precisely the BTZ black brane background (67) introduced earlier,

$$dS^2 = \frac{l_{\text{AdS}}^2}{z^2} \left( - \left( 1 - \left( \frac{z}{b} \right)^2 \right) dt^2 + \frac{dz^2}{1 - \left( \frac{z}{b} \right)^2} + dx^2 \right), \quad (84)$$

where  $x \in \mathbb{R}$ ,  $z \in (0, b]$  and  $z = b$  corresponds to the planar horizon. For simplicity, we compute only one side (+ or -) of the brane, since the other side follows analogously, and the corresponding charge density vectors  $\vec{j}^0$  can be smoothly connected at  $z = b$ . Then, we place a stationary string stretched along the  $z$ -direction, corresponding to the static gauge choice

$$X^t(\tau, \sigma) = \tau, \quad X^z(\tau, \sigma) = \sigma, \quad X^x(\tau, \sigma) = 0. \quad (85)$$

In this gauge, the only non-vanishing current component from the source term (77) is

$$j^{0z} = \frac{z^3}{l_{\text{AdS}}^3} \delta(x), \quad 0 \leq z \leq b. \quad (86)$$

Now consider  $\mathcal{N}$  multiple parallel open strings uniformly distributed along the  $x$ -direction [30, 31, 32]. This modifies the current to

$$j^{0z} = \frac{z^3}{l_{\text{AdS}}^3} \sum_{n \in \mathbb{Z}} \delta(x - nd_s), \quad (87)$$

where  $d_s$  is the separation between adjacent strings. The sum  $\sum_n \delta(x - nd_s)$ , which defines the Dirac comb (or Sha function), indicates that the strings are located at positions  $(\dots, -2d_s, -d_s, 0, d_s, 2d_s, \dots)$ . To prepare for the comparison with bit threads in the next section, let us recall that the threads originate from the boundary region  $A \in [-b, b]$  and end on the complementary region  $B \in (-\infty, b) \cup (b, +\infty)$ . A consistent way to discretize this setup with open strings is to place  $\mathcal{N}$  parallel strings uniformly across the interval of length  $2b$ . The separation between adjacent strings is then

$$d_s = \frac{2b}{\mathcal{N}}. \quad (88)$$

With this choice, the charge density  $j^{0z}$  can be expressed as

$$j^{0z} = \frac{1}{d_s} d_s \frac{z^3}{l_{\text{AdS}}^3} \sum_{n \in \mathbb{Z}} \delta(x - nd_s) = \frac{1}{2b} \frac{z^3}{l_{\text{AdS}}^3} d_s \sum_{n \in \mathbb{Z}} \delta(x - nd_s), \quad (89)$$

where in the second equality the factor of  $\mathcal{N}$  is canceled against the  $1/\mathcal{N}$  in the string coupling (81), so we suppress it here. In the continuum limit,  $\mathcal{N} \rightarrow \infty$  (hence  $d_s \rightarrow 0$ ), the discrete comb of delta functions converges weakly to the constant function 1, yielding the uniform distribution

$$j^{0z} = \frac{1}{2b} \frac{z^3}{l_{\text{AdS}}^3} \lim_{d_s \rightarrow 0} d_s \sum_n \delta(x - nd_s) = \frac{1}{2b} \frac{z^3}{l_{\text{AdS}}^3}. \quad (90)$$

We emphasize that this equality holds distributionally in the  $x$ -direction, not pointwise. The passage from the Dirac comb to a constant function is analogous to techniques in string cosmology, where a single fundamental string is generalized to a gas of  $\mathcal{N}$  strings and the delta-function sources are averaged [75, 76, 77]. In that context, the total energy density of the string gas is obtained by multiplying the number density of strings per spatial volume with the corresponding single-string energy. Moreover, this corresponds to the large- $\mathcal{N}$  decoupling limit in AdS/CFT [50], where  $\mathcal{N}$  denotes the number of branes. Returning to our case, the resulting current density vector is

$$j^{0a} = (j^{0t}, j^{0z}, j^{0x}) = \frac{1}{2b} \frac{z^3}{l_{\text{AdS}}^3} (0, 1, 0), \quad a = t, z, x, \quad (91)$$

which satisfies the 3D divergenceless condition  $\partial_\mu (\sqrt{-g} j^{0a}) = 0$ . To compare with bit threads, we restrict to the 2D time slice  $(z, x)$ . The projected divergenceless condition is

$$\partial_i \left( \sqrt{h^{(2)}} j^{0i} \right) = 0, \quad i = z, x, \quad (92)$$

where the induced current on the time slice of the background is

$$j^{0i} = \sqrt{-g_{tt}} j^{0i} = \frac{1}{2b} \frac{z^2}{l_{\text{AdS}}^2} \sqrt{1 - \left(\frac{z}{b}\right)^2} (1, 0), \quad (93)$$

This describes the Kalb–Ramond charge density vector flowing from  $z = 0$  to  $z = b$ , as depicted in figure (8). Mapping this configuration to figure (9) via the coordinate transformations (72), we obtain

$$v^i = \frac{l_{\text{AdS}}}{2G_N^{(3)}} j^{0i} = \frac{1}{4G_N^{(3)}} \frac{1}{l_{\text{AdS}}} \left( \frac{2bw}{\sqrt{(b^2 - y^2 - w^2)^2 + 4b^2w^2}} \right)^2 \left( \frac{b^2 - y^2 + w^2}{2b}, \frac{yw}{b} \right), \quad (94)$$

where the dimensionless prefactor  $l_{\text{AdS}}/2G_N^{(3)}$  is introduced to normalize the vector  $\vec{j}^0$  such that  $v$  saturates the max-flow min-cut bound  $|v| \leq 1/4G_N^{(3)}$ . This expression exactly reproduces the bit thread vector field obtained earlier [33, 78]. It is worth noting that, when considering the full solutions for  $+$  and  $-$ , the normal flux matches on both sides of the sewing line at  $z = b$ . With boundary conditions, this makes the stitched flow divergenceless. In other words, the flow can not stop at the brane.

Finally, a natural question is whether parallel strings would interact and annihilate. To address this, we must include the missing equation of motion from (76), obtained by varying the string embedding field  $X(\tau, \sigma)$ :

$$\nabla_m (\gamma^{mn} \nabla_n X^a) = -\Gamma_{bc}^a \partial_m X^b \partial_n X^\rho \gamma^{mn} + \frac{1}{2} H_{bc}^a \partial_m X^b \partial_n X^c \epsilon^{mn}. \quad (95)$$

Consider two adjacent strings: one taken as the source (at the origin) and the other a stationary test string placed at some finite separation, both stretched along the  $z$ -direction with the same orientation. Using conformal gauge  $X^0 = \tau$ ,  $X^z = \sigma$ ,  $\gamma^{mn} = \text{diag}(-1, 1)$ ,  $\epsilon^{0z} = 1$  for the test string and the EOM (95), we will get the acceleration for the test string in the transverse direction:

$$\frac{d^2}{d\tau^2} X^x \neq 0. \quad (96)$$

This result implies that the contribution of the graviton to the force between two parallel strings cannot be cancelled by the contribution of the Kalb–Ramond field. In other words, the parallel strings in our case break the no-force condition and inevitably interact with each other as time evolves. This can be understood intuitively: at an initial moment, our setup of parallel strings corresponds to a configuration of bit threads, from which the associated RT surface can be simultaneously determined. Once time evolution is turned on, the strings begin to interact, rearrange, and consequently redefine both the bit threads and the RT surface, since the *entangling regions vary dynamically* with time. This key feature distinguishes our setup from the conventional no-force condition and explains why the latter is violated in our case. A familiar example is the phase transition of the EWCS: when two entangled regions  $A$  and  $B$  evolve to become sufficiently far apart, the EWCS between  $A$  and  $B$  vanishes, splitting into two distinct systems, while a new EWCS between regions  $C$  and  $D$  emerges. This observation is also consistent with our earlier result in string field theory [14], where open string scattering was shown to correspond to the evolution of the entanglement wedge.

### 4.3 Correspondence between string theory and entanglement entropy

Before proceeding to further analysis, let us pause briefly to summarize the results obtained thus far. Based on the previous observations, the correspondence between the string worldsheet and the RT surface becomes manifest. The internal consistency of the worldsheet theory requires the action to include not only the symmetric spacetime metric  $g_{ab}$  but also the antisymmetric Kalb–Ramond field  $B_{ab}$  and the constant dilaton  $\phi$ . All three fields are indispensable:

1. Since our constructed action locally reduces to the Polyakov action (48) of string worldsheet theory, its equations of motion admit the  $\text{AdS}_3$  solution if and only if both  $g_{ab}$  and  $B_{ab}$  are included simultaneously.
2. The constant dilaton  $\phi$  ensures the string coupling remains weak,  $g_s \ll 1$ . Consequently, multiple string sources do not backreact on the  $\text{AdS}_3$  geometry at leading order, allowing us to establish a consistent correspondence between the string charge density and the bit threads in  $\text{AdS}_3$ .

Moreover, since entanglement entropy can be computed using the spacetime metric  $g_{ab}$ , it is natural to expect that there exists a comparable entanglement-related quantity computable via the Kalb–Ramond field  $B_{ab}$ . This theoretical requirement provides compelling evidence in support of the bit thread formulation of entanglement entropy. Consequently, it enables us to establish an explicit correspondence between quantities in the worldsheet theory and those in entanglement entropy, as illustrated in figure (10):

Worldsheet	Entanglement
$D$ -brane/ $E$ -brane	RT surface
Charge density vector $\vec{j}^0$	Bit threads $v$

Under this setup, the left-hand panel illustrates the oriented blue lines in figure (10), which represent the Kalb–Ramond charge density vector  $\vec{j}^0$ , tangent to the string. Specifically, this vector lies along the string in the direction of increasing  $\sigma$ , reflecting the string’s orientation. The red curve in the same panel depicts the geodesic trajectory of a string endpoint, corresponding to a  $D$ -brane. This  $D$ -brane thus plays the role of the entangling surface, or more precisely, the entangling brane ( $E$ -brane) [37]. This result agrees with earlier studies, particularly when one considers extending the open string beyond the  $D$ -brane, effectively slicing it into two parts [9, 37]. It is also consistent with understanding from loop quantum gravity [79]. In this configuration, entanglement entropy arises from tracing out the degrees of freedom on one side of the  $D$ -brane, and its value is proportional to the area (length, in this case) of the brane. This correspondence is illustrated in the left and right panel of figure (10). Moreover, given that  $g_{ab}$  and  $B_{ab}$  appear on equal footing in the worldsheet action, their dual quantities in the entanglement entropy framework—namely, the RT surface and the bit threads—should likewise be treated on an equal footing. Remarkably, this expectation is realized: entanglement entropy can indeed be computed through both the geodesic length of the RT surface and the flux of bit threads:

$g_{ab}$	RT surface	$S_{vN} = \frac{\text{area}(\gamma_A)}{4G_N}$
$B_{ab}$	Bit threads $v$	$S_{vN} = \max_v \int_A v$

The computational setup for evaluating entanglement entropy using bit threads is visually illustrated in the right-hand panel of figure (10).

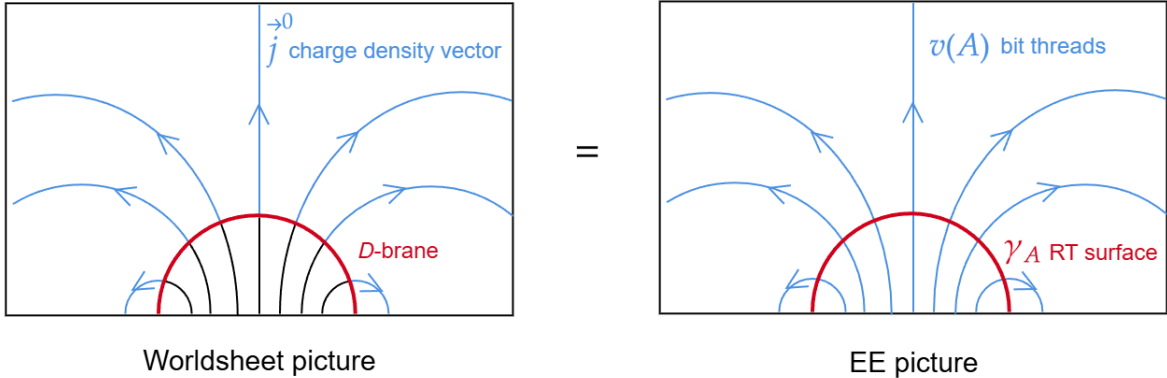


Figure 10: This figure illustrates the correspondence between the worldsheet formulation and the entanglement entropy framework. In this picture, the  $D$ -brane is identified with the RT surface  $\gamma_A$  on a time slice of  $\text{AdS}_3$ . To realize the  $\text{AdS}_3$  background from string theory, the inclusion of the Kalb–Ramond field is essential. This field gives rise to the Kalb–Ramond charge density vector  $\vec{j}^0$ , which is tangent to the open string parameterized from  $\sigma = 0$  to  $\pi$ . Notably, this vector is orthogonal to the  $D$ -brane and corresponds to the bit thread vector  $v(A)$ , which is orthogonal to the RT surface  $\gamma_A$ . Both  $\vec{j}^0$  and  $v(A)$  satisfy a divergenceless condition,  $\nabla \cdot \vec{j}^0 = \nabla \cdot v = 0$ , reinforcing the parallel between the string worldsheet description and the bit thread formulation of entanglement entropy.

On the other hand, it is worth noting that this correspondence explicitly demonstrates that space-time geometry and dynamics are determined jointly by entanglement entropy (via the RT surface) and bit threads, since the equations of motion are those of  $g_{ab}$  and  $B_{ab}$ . Because the bit-thread flow  $v$  necessarily incorporates the RT surface, which connects the UV and IR regions, this provides a verification of our earlier conjecture that bulk geometries can be fixed by two distinct kinds of entanglement entropies: one defined by RT surfaces whose endpoints both lie on the AdS boundary, and the other defined by surfaces with one endpoint anchored on the boundary and the other extending into the deep bulk [80, 81, 82].

Finally, our discussion has primarily focused on open strings. For closed strings, the corresponding construction can be obtained through a quotient procedure or the replica "copy-and-glue" method, as in the case of reflected entropy on ordinary manifolds [16]. In such scenarios, the geodesic supporting the D-brane corresponds to the initial and final configurations of the closed string worldsheet. We will present a concrete example of closed string case in the next section.

## 5 Novel results

In the previous section, we established an explicit correspondence between the string worldsheet and the RT surface. One may naturally ask whether this correspondence yields any novel or previously unknown results. In this section, we will present some of them.

### 5.1 Computing entanglement entropy from open string charge

Remarkably, if the correspondence holds, it offers a new method to compute the entanglement entropy of a  $CFT_2$  using string-theoretic quantities.

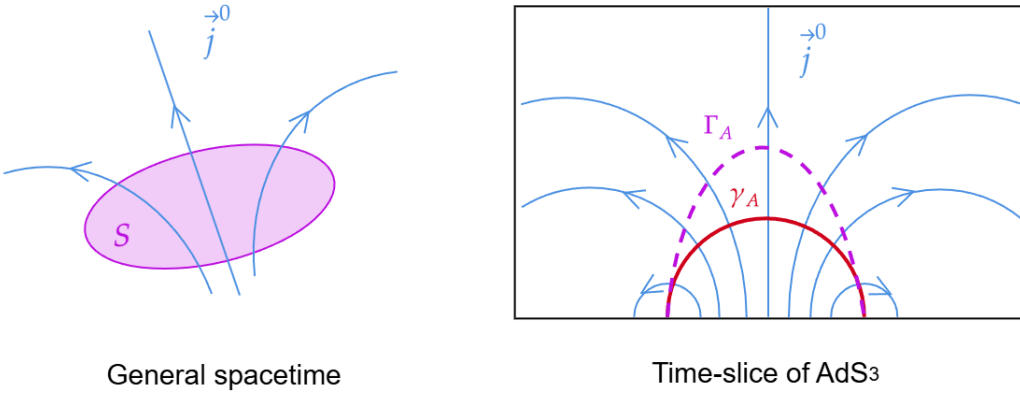


Figure 11: This figure illustrates the definition of the string number  $\mathcal{N}$ . In the left-hand panel, for a general spacetime, the two-dimensional surface  $S$  is pierced by open strings, and the string number is defined via the integration of the string charge density vector  $\vec{j}^0$  across  $S$ . In the right-hand panel, we depict the specific case relevant to our discussion: the time slice of  $AdS_3$ , where the surface  $S$  reduces to a one-dimensional curve  $\Gamma_A$ . When  $\Gamma_A$  coincides with the geodesic  $\gamma_A$  on which the  $D$ -brane resides, the charge density vectors  $\vec{j}^0$  become normal to  $\gamma_A$ .

To explore this, we recall a key observable in string theory—the *string number*  $\mathcal{N}$  [83], which can be expressed in terms of the open string charge density. Concretely, it is defined via the Kalb–Ramond charge density vector  $\vec{j}^0$  as

$$\mathcal{N} \equiv \int_S \vec{j}^0 \cdot d\vec{a}. \quad (97)$$

where  $S$  is a two-dimensional surface pierced by strings, and the integrand counts the net flux of strings through  $S$ , as illustrated in figure (11). Note that the string number  $\mathcal{N}$  defined here differs from its conventional definition. Since  $\vec{j}^0$  is obtained by summing over all parallel stationary strings in (90),  $\mathcal{N}$  is no longer a discrete quantity but instead takes continuous values. On a time slice of  $AdS_3$ , this reduces to an integral over a one-dimensional curve  $\Gamma_A$ . Using the previous results (94), the string number becomes

$$\mathcal{N} = \int \vec{j}^0 \cdot dS_{\Gamma_A} = \frac{2G_N^{(3)}}{l_{\text{AdS}}} \int \vec{v} \cdot dS_{\Gamma_A}, \quad (98)$$

where  $\Gamma_A$  is any curve homologous to the entangling region  $A$  on the conformal boundary. When  $\Gamma_A$  coincides with the geodesic  $\gamma_A$  on which the  $D$ -brane resides, the vector  $\vec{j}^0$  becomes the unit normal  $\hat{n}$  to the  $D$ -brane. Then, the integral simplifies to

$$\mathcal{N} = \frac{2G_N^{(3)}}{l_{\text{AdS}}} \int \vec{v} \cdot dS_{\Gamma_A} = \frac{2G_N^{(3)}}{l_{\text{AdS}}} \int \vec{n} \cdot dS_{\gamma_A} = \frac{1}{2} \frac{L_{\gamma_A}}{l_{\text{AdS}}}, \quad (99)$$

where  $L_{\gamma_A}$  is the geodesic length. This allows us to directly relate the entanglement entropy of region  $A$  to the string number by using the previous results (94) and (99):

$$S_{\text{vN}} = \frac{L_{\gamma_A}}{4G_N^{(3)}} = \frac{l_{\text{AdS}}}{4G_N^{(3)}} \cdot 2\mathcal{N} = \frac{c}{3} \ln \left( \frac{2b}{\epsilon} \right), \quad (100)$$

where  $\epsilon$  is UV cut-off and central charge  $c = 3l_{\text{AdS}}/2G_N^{(3)}$ . This result carries significant conceptual implications:

- The entanglement entropy arises from the number of open strings piercing the entangling surface (i.e., the  $D$ -brane).
- Each open string, endowed with a unit of Kalb–Ramond charge, contributes a single bit of information. This bit encodes a microstate associated with the entangling region  $A$  and is stored holographically on the entangling surface  $\gamma_A$ .

## 5.2 Computing Bekenstein–Hawking entropy from closed string charge

In the previous section, we derived the entanglement entropy using open string charge. We now turn to the Bekenstein–Hawking entropy of the BTZ black hole, deriving it through closed string charge. This approach provides new insight into the conjecture proposed by Susskind and Uglum.

To begin, let us recall the thermofield double (TFD) formalism and its holographic interpretation [84, 85]. The total Hilbert space is given as the tensor product of two identical CFT Hilbert spaces,

$$\mathcal{H}_{\text{total}} = \mathcal{H}_A \otimes \mathcal{H}_B, \quad (101)$$

where each energy eigenstate satisfies  $H|n\rangle = E_n|n\rangle$ . The TFD state, a pure entangled state in this doubled system, is defined as

$$|TFD\rangle = \frac{1}{\sqrt{Z(\beta)}} \sum_n e^{-\beta E_n/2} |E_n\rangle_A \otimes |E_n\rangle_B, \quad Z(\beta) = \sum_n e^{-\beta E_n}, \quad (102)$$

where  $T = 1/\beta$  is the temperature. The corresponding density matrix takes the form

$$\rho_{\text{total}} = |TFD\rangle \langle TFD|. \quad (103)$$

The entropy of subsystem  $A$  coincides with the entanglement entropy between the two CFT copies,

$$S_A = -\text{tr} \rho_A \ln \rho_A, \quad (104)$$

where the reduced density matrix is  $\rho_A = \text{tr}_B \rho_{\text{total}} = e^{-\beta H_A}$ . Once the TFD state is specified, the entangling regions  $A$  and  $B$  can be chosen on each respective boundary, and the entanglement entropy  $S_A$  can be computed using equation (104), as illustrated in the two right panels of figure (12).

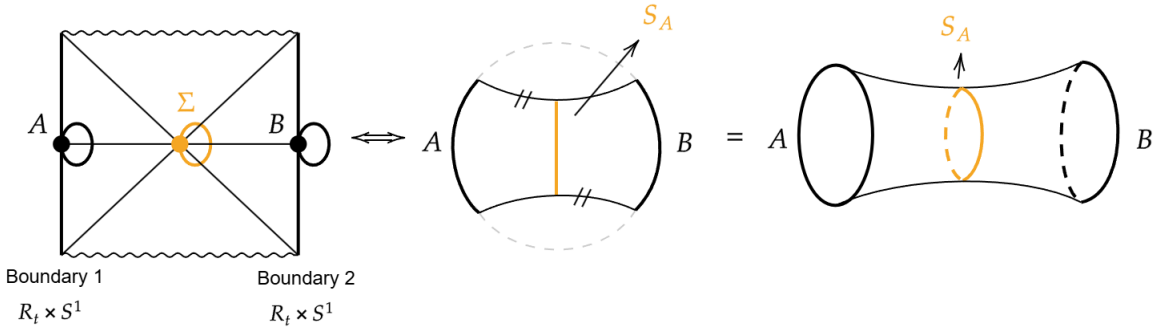


Figure 12: This figure illustrates the holographic interpretation of the TFD state. In the first panel, each point along the central horizontal line represents an  $S^1$  circle. The midpoint of this line, marked by the orange circle, corresponds to the event horizon  $\Sigma$  at  $t = 0$  of the BTZ black hole. This horizontal line can be reinterpreted as shown in the second and third panels, where the orange geodesics denote the RT surface. The third panel is obtained as a quotient of the geometry depicted in the second panel. Notably, the event horizon and the RT surface coincide, capturing the same surface.

Holographically, the TFD state corresponds to the two-sided asymptotic boundaries of the maximally extended Penrose diagram of the BTZ black hole [86]. Each point in this diagram represents a spatial  $S^1$  circle, as shown in the left panel of figure (12). At fixed time, the entangling regions  $A$  and  $B$  are located on the boundary endpoints of the horizontal line. The entanglement entropy  $S_A$ , computed from the CFT equation (104), exactly reproduces the area of the central orange point on this line, which coincides with the area of the BTZ event horizon  $\Sigma$ . Consequently, the entanglement entropy and the Bekenstein–Hawking entropy describe the same surface [87],

$$S_A = S_{BH} = \frac{2\pi r}{4G_N^{(3)}}. \quad (105)$$

Therefore, once we obtain the length of the orange circle, we can directly compute the Bekenstein–Hawking entropy of the black hole. Let us now return to the open string case, where the string carries the Kalb–Ramond charge. When the background shown in figure (13) is compactified by the quotient, we can invoke the open–closed string duality. Under this duality, the open string charge maps to the closed string charge. The corresponding charge flow precisely winds around the orange circle, reproducing its area. If this interpretation is correct, the Bekenstein–Hawking entropy of the BTZ black hole can indeed be computed from the closed string charge.

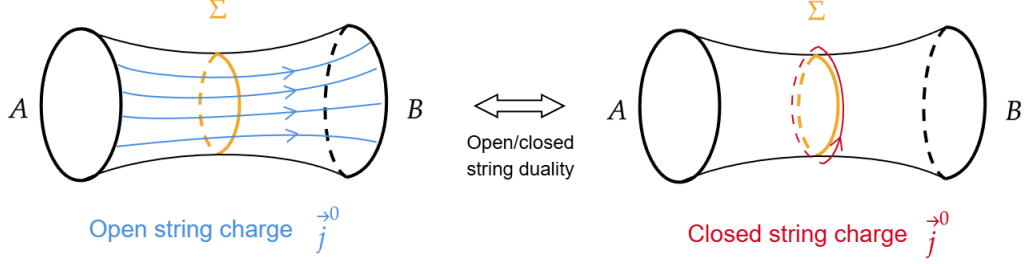


Figure 13: This picture illustrates the open–closed string duality in terms of the configuration of string charge density. After taking the quotient of the geometry, the open string charge can be interpreted as the current flowing from region  $A$  to region  $B$ . Its closed string dual corresponds to the current circulating around the non-contractible circle, thereby producing a non-vanishing total closed string charge. This closed string charge precisely encodes the radius of the compactified circle, which is identified with the horizon of the BTZ black hole.

To verify this idea, let us first recall the definition of the total string charge  $\vec{Q}$ , given as the spatial integral of the string charge density [83]:

$$\vec{Q} = \int d^d x \sqrt{h^{(d)}} \vec{j}^0. \quad (106)$$

Since  $\vec{j}^0$  is defined by equations (77) and (93), in the background (84) the factor  $\sqrt{h^{(2)}}$  cancels out, leaving the closed string charge

$$\vec{Q} = \int_0^{2\pi} d\sigma \partial_\sigma \vec{X}(t_0, \sigma). \quad (107)$$

For a contractible closed string, the total charge vanishes due to  $\vec{Q} = \vec{X}(t_0, 2\pi) - \vec{X}(t_0, 0) = 0$ . In contrast, for a non-contractible closed string winding around the compactified dimension  $x$ , the total charge is nonzero. Parameterizing the embedding as  $X = r\sigma$ , where  $r$  denotes the radius of the compactified circle, we obtain

$$\vec{Q} = (0, Q), \quad Q = 2\pi r. \quad (108)$$

The Bekenstein–Hawking entropy is then given by

$$S_{BH} = \frac{Q}{4G_N^{(3)}} = \frac{2\pi r}{4G_N^{(3)}}, \quad (109)$$

which exactly reproduces the Bekenstein–Hawking entropy (105) of BTZ black hole. This result leads to two key implications:

- The Bekenstein–Hawking entropy can be expressed in terms of the closed string charge.

- In higher dimensions, the corresponding generalization is provided by D-brane charges, which naturally account for the entropy of higher-dimensional black holes.

We believe this provides the most straightforward explanation of the Bekenstein–Hawking entropy for the D1–D5 black hole system [70, 71, 72]. The corresponding Bekenstein–Hawking entropy is given by  $S_{BH} = 2\pi\sqrt{Q_1 Q_5 N}$ , where  $Q_1$ ,  $Q_5$  and  $N$  are three different charges: the wrapping number of the D1-branes, the wrapping number of the D5-branes, and the momentum quantum number, respectively. This entropy can also be captured by entanglement entropy. The near-horizon geometry of the D1–D5 black hole is given by  $BTZ_3 \times S^3 \times T^4$ , and in the near-horizon limit of a near-extremal  $BTZ_3$  black hole, the geometry reduces to  $AdS_2 \times S^1$ . In this case, the corresponding thermofield double (TFD) state in the  $AdS_2/CFT_1$  correspondence can also be used to compute the entanglement entropy [88]. Therefore, the equivalence between the Bekenstein–Hawking entropy and entanglement entropy in this setting provides further evidence for our earlier result that these two entropies represent the same physical quantity, related by open–closed string duality. Related discussions can also be found in [89].

Finally, the entanglement entropy and the Bekenstein–Hawking entropy, computed from the open and closed string charges, provide a new avenue to verify the conjecture of Susskind and Uglum. We will elaborate on this explanation within the framework of the Susskind–Uglum conjecture in Section 5.4.

### 5.3 ER=EPR from the string perspective

We can now revisit the ER = EPR conjecture from the perspective of string theory, building on our previous results. We begin by revisiting Van Raamsdonk’s thought experiment. In the  $AdS/CFT$  correspondence, if two subsystems are completely unentangled, their joint state is simply a product state,

$$|\Psi\rangle = |\Psi_A\rangle \otimes |\Psi_B\rangle. \quad (110)$$

which corresponds to two disconnected spacetimes, with each  $\Psi_i$  dual to the geometry of the respective subsystem. Once the two subsystems are entangled, however, the product state is replaced by the TFD state,

$$|\text{TFD}\rangle = \sum_n e^{-\beta E_n/2} |E_n\rangle_A \otimes |E_n\rangle_B, \quad (111)$$

where  $\beta$  is the inverse temperature and  $E_n$  are energy eigenvalues. The TFD state may be viewed as a quantum superposition of disconnected geometries, which effectively yields a connected spacetime—such as a wormhole—illustrated in figure (14).

This interplay between entanglement and geometry underlies the ER=EPR conjecture, which posits that quantum entanglement (EPR pairs) is associated with the formation of Einstein–Rosen (ER) bridges. In the zero-temperature limit  $\beta \rightarrow \infty$ , the entangled TFD state reduces to the unentangled product state, and the wormhole disappears. In this regime, the wormhole horizon area shrinks to zero while its proper length diverges, consistent with Raamsdonk’s argument and depicted in figure (15).

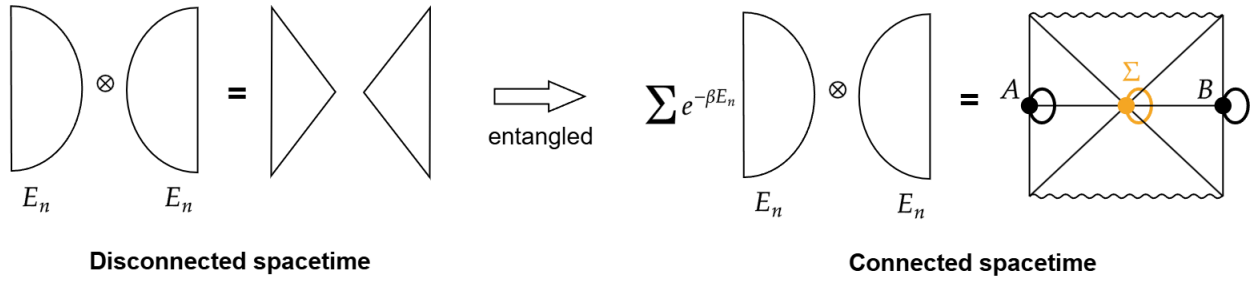


Figure 14: This picture illustrates Van Raamsdonk’s argument. The left panel shows that when the two subsystems are not entangled, the bulk interpretation corresponds to a disconnected spacetime. In contrast, the right panel shows that when the two subsystems are entangled, a connected spacetime emerges through the quantum superposition of disconnected geometries.

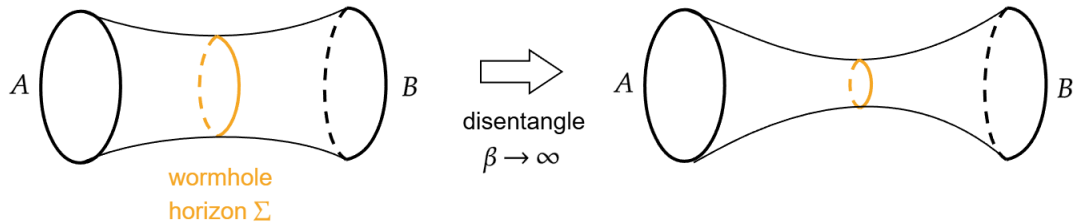


Figure 15: Illustrating the disentanglement in the bulk dual of the TFD. As the entanglement between subsystems  $A$  and  $B$  decreases to zero, the area of the minimal surface  $\Sigma$  (the wormhole horizon) separating the two regions also shrinks to zero. Correspondingly, the proper distance between the associated bulk regions diverges. In this limit, the spacetime regions are pulled apart and eventually pinch off from one another, resulting in disconnected geometries.

Since entanglement entropy can be realized in our proposed string worldsheet picture, it follows naturally that there exists a string-theoretic version of ER = EPR. In this picture, the closed string winds around the wormhole horizon, with its winding charge contributing directly to the Bekenstein–Hawking entropy. As the entanglement entropy between two subsystems  $A$  and  $B$  decreases, the corresponding bulk horizon shrinks.

When the horizon radius falls below the string length scale, the winding closed string develops tachyonic modes. This may trigger closed string tachyon condensation, potentially reducing the total winding charge  $Q$  toward zero. It is important to emphasize that this process closely parallels the mechanism of topology change via closed string winding tachyons studied in [90]. The crucial difference is that, in our setup, the shrinking of the radius is not driven by a one-loop effective potential that destabilizes the modulus. Instead, it arises dynamically through disentanglement in the dual CFT. A vanishing or suppressed  $Q$  would then suggest that the winding mode becomes effectively contractible,

indicating a possible transition where the originally connected spacetime with a finite compact dimension could fragment into two disconnected components, as illustrated in figure (16). While this scenario is consistent with known results on closed string tachyon condensation, here we present it as a conjectural realization of ER=EPR in the  $\text{AdS}_3/\text{CFT}_2$  framework. Thus, closed string tachyon condensation provides a natural microscopic mechanism for the disentanglement process in the ER = EPR framework. This observation reinforces our earlier claim that entanglement entropy can serve as a probe of the closed string tachyon vacuum in closed string field theory [13, 14].

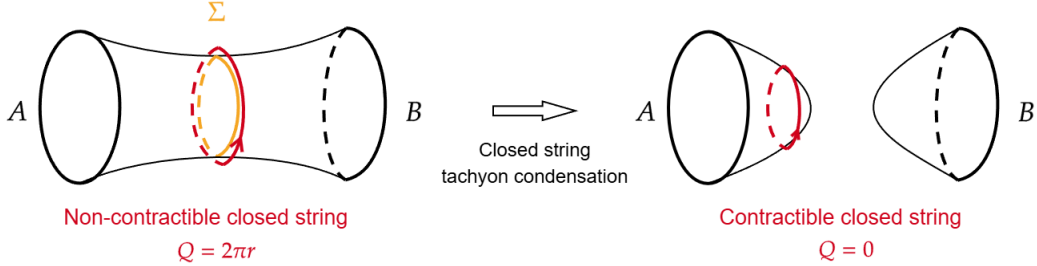


Figure 16: We begin with a closed string winding around the wormhole horizon in our proposed configuration. The topological change of the wormhole proceeds in three steps: (1) Disentanglement between the two subsystems, which reduces the horizon size; (2) once the horizon shrinks below the string length scale, the winding closed string becomes tachyonic; (3) finally, tachyon condensation drives the closed string charge  $Q = 0$ , signaling that the spacetime splits into two disconnected components.

Recent studies on the relation between quantum extremal surfaces and the island formula using replica wormholes can be found in [91]. It was further shown that the replica wormhole and the island formula can be derived directly from CFT [92]. A comprehensive review of recent developments on wormholes in holography is provided in [93].

#### 5.4 New realization of Susskind and Uglum's conjecture

In this subsection, we aim to extend the understanding of Susskind and Uglum's conjecture in light of our previous results. In Susskind and Uglum's framework, black hole entropy naturally arises in string theory. The sphere diagram accounts for the classical Bekenstein–Hawking entropy of a black hole: it may be interpreted as a closed string emitted from one point on the horizon and reabsorbed at another. Equivalently, it corresponds to the one-loop diagram of open string theory, with both endpoints anchored on the horizon, as illustrated in figure (1). This dual interpretation reflects the open–closed string duality, where the one-loop open string diagram and the two-punctured closed string sphere share the same underlying Riemann surface. Our results refine this picture in the context of  $\text{AdS}_3/\text{CFT}_2$ , as illustrated in figure (17).

In this setting, the two-punctured sphere is naturally replaced by the hyperbolic cylinder. Consequently, the entangling surface is no longer represented by two punctures but instead sits at the waist of the hyperbolic cylinder: in the open string picture, strings pass through the horizon, while in the

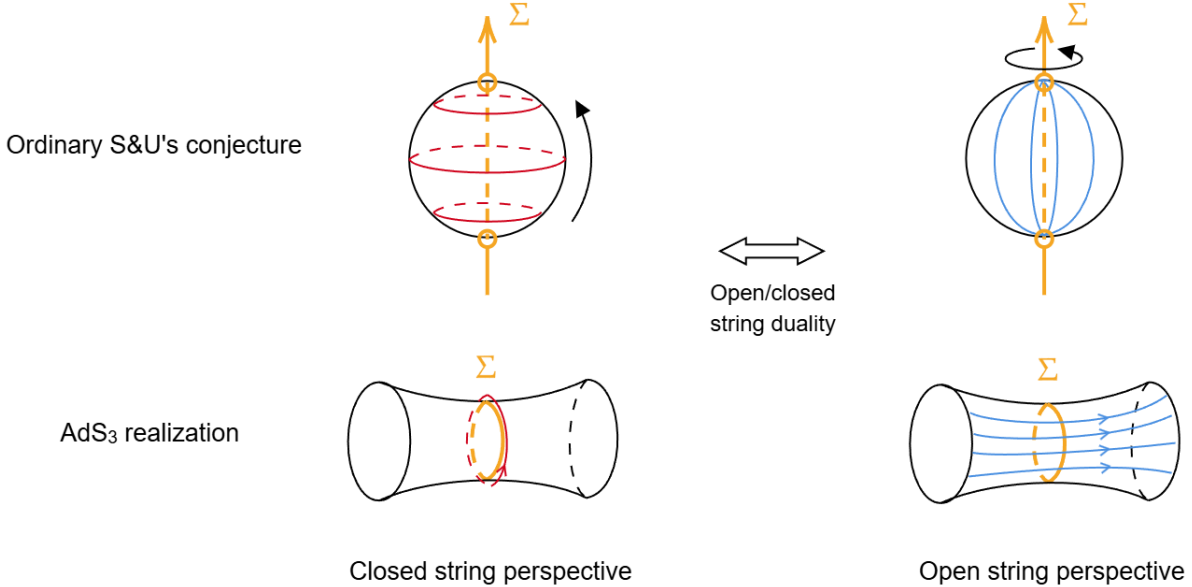


Figure 17: This figure illustrates how the Susskind–Uglum conjecture can be generalized to the  $\text{AdS}_3/\text{CFT}_2$  framework. In our proposed configuration, the two-punctured spheres of the original Susskind–Uglum setup (shown in the first row) are replaced by hyperbolic cylinders in  $\text{AdS}_3$  (shown in the second row). The open– and closed–string descriptions extend naturally to the cylinder geometry. In this context, the entangling surface or horizon, which punctures the two-sphere in the original picture, is realized as the waist of the hyperbolic cylinder in  $\text{AdS}_3$ , corresponding to the throat of the wormhole.

closed string picture, they wind around it. This modification both confirms and sharpens the Susskind–Uglum conjecture, as we demonstrated that open string charge contributes to entanglement entropy, whereas closed string charge contributes to black hole entropy. Furthermore, since our construction can be naturally extended to the ER=EPR framework, we arrive at an equivalent interpretation in which entanglement and geometry are unified through string-theoretic charges, as illustrated in figure (18).

Obviously, this equivalence naturally shares the same underlying property. To see this, let us first recall the open–closed string duality. In string theory, the appropriate description of the string cylinder—either as a one-loop open string stretched between D-branes or as a tree-level closed string exchanged in the bulk—depends on the brane separation. When the separation is large, the propagation of closed strings dominates at long distances: the massive modes decouple, leaving only the massless sector. However, the corresponding open strings are long, so their massive excitations significantly contribute, leading to strong gauge coupling. Conversely, when the D-branes are close together, the supergravity approximation breaks down, while the massless sector of open strings dominates. Thus, as the D-brane separation increases, the open string description is gradually replaced by the closed string description, and the two descriptions ultimately become causally disconnected as the closed-string

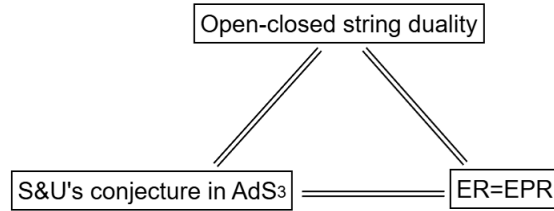


Figure 18: This figure illustrates the equivalence between open–closed string duality, ER=EPR, and the Susskind–Uglum conjecture.

propagation time tends to infinity.

A similar mechanism emerges in the other two frameworks we have discussed. In the ER=EPR context, the degree of quantum entanglement plays the role of the brane separation: strongly entangled states correspond to a connected wormhole geometry, while weak entanglement invalidates the usual von Neumann entropy measure, requiring instead a description in terms of black hole entropy. When the systems become completely disentangled, the wormhole throat shrinks to zero and the spacetimes disconnect, reflecting a transition in the dominant description. Likewise, in the EWCS, phase transitions occur when tuning the size or separation of subsystems, with different extremal surfaces controlling the entropy in different regimes. Finally, the Susskind–Uglum conjecture can also be understood within this duality structure: black hole entropy admits both a microscopic entanglement interpretation and a macroscopic geometric area law, with the relevant description depending on the physical regime.

Taken together, these parallels suggest that open–closed string duality, ER=EPR, and the Susskind–Uglum conjecture are not merely analogous but manifestations of a deeper equivalence. In each case, the transition between dual descriptions—whether in string theory, spacetime geometry, or entanglement entropy—reflects the same underlying principle.

Finally, we also wish to emphasize the distinction between the method used in the ordinary Susskind–Uglum conjecture and our picture in  $\text{AdS}_3$ . In the original Susskind–Uglum setup, the compact spherical worldsheet intersects the horizon infinitely many times. The reason is that the worldsheet field  $X^\mu$  exhibits short-distance quantum fluctuations [94, 95]. Consequently, an unregulated ( $\epsilon = 0$ ) spherical worldsheet cannot intersect the horizon at only two points. This leads directly to the problem that the punctured-sphere partition function cannot be defined. To address this issue, off-shell string theory introduces a UV regulator  $\epsilon$ ; see [11] for details. In contrast, in our work the entropy is computed from the string number, which is determined by the number of strings—each carrying Kalb–Ramond charge—that cross the horizon at any fixed time slice. From this viewpoint, although a single macroscopic string may intersect the horizon infinitely many times due to short-distance fluctuations, the total number of strings remains well-defined and unique as long as the parallel strings do not interact. This is precisely why our approach differs conceptually from the off-shell sphere-partition-function

method and avoids the necessity of introducing a UV regulator.

## 5.5 Are the entanglement entropy and RT surface quantized?

In the previous discussion, we considered multiple parallel open strings carrying Kalb–Ramond charge, each contributing to the entanglement entropy. A natural question arises: if we consider only a single string, does it correspond to one quantum of entanglement entropy—i.e. to the minimal “bit” of entanglement? Since the entanglement entropy is proportional to the area of the RT surface, this would suggest that the RT surface itself possesses a minimal value and is quantized.

To examine this, let us recall the charge density vector for a single string source,

$$j^{0a} = (j^{0t}, j^{0z}, j^{0x}) = \frac{z^3}{l_{AdS}^3} (0, \delta(x), 0), \quad 0 \leq z \leq b. \quad (112)$$

As in our earlier argument, we consider the induced current on the time slice of the background,

$$j^{0i} = \sqrt{-g_{tt}} j^{0i} = \frac{z^2}{l_{AdS}^2} \sqrt{1 - \left(\frac{z}{b}\right)^2} (\delta(x), 0), \quad i = z, x. \quad (113)$$

Performing the coordinate transformation (we restrict attention to the + branch)

$$y = \frac{b \sinh(x/b)}{\cosh(x/b) + \sqrt{1 - (z/b)^2}}, \quad w = \frac{z}{\cosh(x/b) + \sqrt{1 - (z/b)^2}}, \quad (114)$$

with inverse

$$z = \frac{2b^2 w}{\sqrt{(b^2 - y^2 - w^2) + 4b^2 w^2}}, \quad x = \frac{b}{2} \log \left( \frac{(b+y)^2 + w^2}{(b-y)^2 + w^2} \right). \quad (115)$$

the charge density vector becomes

$$\begin{aligned} j^{0y} &= \frac{2yw^2(b^2 + w^2)}{l_{AdS}^2 [(b^2 - y^2 - w^2)^2 + 4b^2 w^2]} \delta(y), \\ j^{0w} &= \frac{w^2(b^2 - y^2 + w^2)(b^2 + w^2)}{l_{AdS}^2 [(b^2 - y^2 - w^2)^2 + 4b^2 w^2]} \delta(y). \end{aligned} \quad (116)$$

Since the delta function enforces  $y = 0$ , this simplifies to

$$(j^{0w}, j^{0y}) = \left( \frac{w^2}{l_{AdS}^2} \delta(y), 0 \right), \quad (117)$$

which lives on the Poincaré patch of a time slice of  $AdS_3$ :

$$dS^2 = \frac{l_{AdS}^2}{w^2} (dy^2 + dw^2). \quad (118)$$

Using the correspondence (94),

$$v = \frac{l_{\text{AdS}}}{2G_N^{(3)}} (j^{0w}, j^{0y}). \quad (119)$$

we compute the entanglement entropy. On a constant  $w$  surface, the induced metric is  $h = \frac{l_{\text{AdS}}^2}{w^2}$ , and the unit normal vector is  $n_\mu = (l_{\text{AdS}}/w, 0)$ . Thus,

$$\sqrt{h} n_\mu v^\mu = \frac{l_{\text{AdS}}}{2G_N^{(3)}} \delta(y) \quad (120)$$

Integrating over the boundary interval,

$$S_{\text{vN}} = \int_A \sqrt{h} n_\mu v^\mu = \int_{\epsilon-b}^{b-\epsilon} \sqrt{h} n_\mu v^\mu dy = \frac{l_{\text{AdS}}}{4G_N^{(3)}} \cdot 2, \quad (121)$$

This exactly matches our earlier result (100) for the entanglement entropy of open strings when  $\mathcal{N} = 1$ . It therefore represents the minimal value of the entanglement entropy and the corresponding minimal length of the RT surface. For a general number  $\mathcal{N}$  of strings, the result extends straightforwardly to

$$S_{\text{vN}} = \frac{l_{\text{AdS}}}{4G_N^{(3)}} \cdot 2\mathcal{N}. \quad (122)$$

Hence, the entanglement entropy is discretized according to the number of strings, providing strong evidence that the RT surface itself should be quantized. In the limit  $\mathcal{N} \rightarrow \infty$  with inter-string spacing  $d_s \rightarrow 0$ ,  $\mathcal{N}$  becomes effectively continuous, and the result reduces to the well-known  $\text{CFT}_2$  entanglement entropy (100).

Based on this observation, the pure state  $|\psi\rangle$  of the two segments of open string,  $\text{string}_1$  and  $\text{string}_2$  on two sides of RT-surface shown in figure (9), can be decomposed as  $|\psi\rangle \in \mathcal{H} \subseteq \mathcal{H}_{\text{string}_1} \otimes \mathcal{H}_{\text{string}_2}$ . Consequently, we obtain

$$\frac{l_{\text{AdS}}}{4G_N^{(3)}} \cdot 2 \widehat{\int_{\gamma_A} \vec{j}^0} |\psi\rangle = \frac{l_{\text{AdS}}}{4G_N^{(3)}} \cdot 2\mathcal{N} |\psi\rangle, \quad (123)$$

where the current  $\vec{j}^0$  is promoted to an operator.

To further substantiate the evidence for the quantization of entanglement entropy and the RT surface, let us revisit our setup, in which an oriented open string is intersected by the RT surface and thereby divided into two segments, as shown in the left panel of figure (19). In this picture, the entanglement entropy (122) naturally measures the quantum correlations between the two string segments. Although the explicit Schmidt decomposition of the open string Hilbert space is technically challenging, the bit-thread formalism provides a well-defined method to compute this entanglement entropy. Interestingly, a closely analogous situation arises in loop quantum gravity (LQG). There, the entangling surface cuts an oriented Wilson line state  $\gamma$  into two parts, as illustrated in the right panel of figure (19). The entanglement entropy between these two parts is known to be quantized, yielding discrete values. This suggests that quantization of entanglement entropy and its dual RT surface may

be natural both in string theory and LQG. It therefore provides a potential bridge between string theory and LQG, realized through the discrete nature of entanglement entropy.

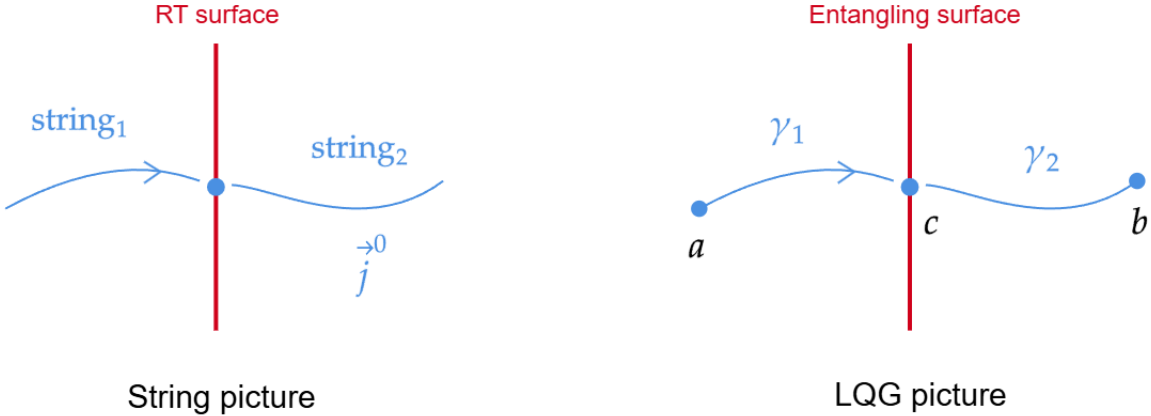


Figure 19: This picture illustrates the similarities between the entanglement entropies obtained from string theory and from LQG. In the string theory picture, the oriented open string charge density  $\vec{j}^0$  crossing the RT surface (or D-brane) contributes to the minimal value of entanglement entropy. As the number of open strings increases, the entanglement entropy and the area of the RT surface both increase in discrete steps. In the LQG picture, the entangling surface cuts the oriented Wilson line into two parts, to which the Schmidt decomposition can be applied. This again yields minimal values of entanglement entropy. As more Wilson lines cross the entangling surface, introducing additional nodes on it, the entanglement entropy and the area of the entangling surface also increase in discrete steps.

To be specific, let us recall the calculation of entanglement entropy in LQG [79]. The first step is to perform a Schmidt decomposition. Our previous study of the TFD state already provides a canonical physical realization of the Schmidt decomposition for thermal states. Consider a region divided into two subregions,  $A$  and  $B$ , by entangling surface. Any pure state  $|\psi\rangle \in \mathcal{H} = \mathcal{H}_A \otimes \mathcal{H}_B$  can be decomposed into a product basis as

$$|\psi\rangle = \sum_i \lambda_i |\varphi_i^A\rangle \otimes |\varphi_i^B\rangle. \quad (124)$$

which is the Schmidt decomposition. Here,  $\lambda_i$  are the Schmidt coefficients and the number of non-zero terms defines the Schmidt rank. Tracing over one subregion gives the reduced density matrix for region  $A$ :

$$\rho(A) = \sum_i \lambda_i^2 |\varphi_i^A\rangle \langle \varphi_i^A|, \quad (125)$$

and similarly for region  $B$ :

$$\rho(B) = \sum_i \lambda_i^2 |\varphi_i^B\rangle \langle \varphi_i^B|. \quad (126)$$

The von Neumann entanglement entropy of either subsystem is then

$$S_{\text{vN}}(A) = S_{\text{vN}}(B) = -\sum_i \lambda_i^2 \log \lambda_i^2. \quad (127)$$

Now, let us see how this decomposition can be used to calculate the entanglement entropy of the simplest spin-network states. We begin by recalling the Wilson line state  $|\gamma, j, a, b\rangle$ . In LQG, such states are functionals that map the  $\mathfrak{su}(2)$  connection  $A$  on a path  $\gamma$  to  $\mathbb{C}$ . Explicitly, the Wilson line state can be written as

$$\psi_{\gamma, j, a, b}[h(A)] = \langle h(A) | \gamma, j, a, b \rangle = \sqrt{2j+1} D_{ab}^{(j)}(h_\gamma(A)), \quad (128)$$

where  $h(A) = \mathcal{P} \exp(\int A)$  denotes the holonomy of the connection along  $\gamma$ , and  $D_{ab}^{(j)}(g)$  are Wigner matrices giving the spin- $j$  irreducible representation of  $g \in SU(2)$ , with matrix indices  $a, b$ . The prefactor  $\sqrt{2j+1}$  ensures orthonormality and proper normalization of the link states. Now suppose the path  $\gamma$  is split into two segments,  $\gamma = \gamma_1 \circ \gamma_2$ , as illustrated in the right panel of figure (19). The corresponding Hilbert space factorizes as

$$\mathcal{H}_\gamma \subseteq \mathcal{H}_{\gamma_1} \otimes \mathcal{H}_{\gamma_2}. \quad (129)$$

Accordingly, the Wilson line state admits the decomposition

$$\begin{aligned} \psi_{\gamma_1 \circ \gamma_2, j, a, b}[h(A)] &= \frac{1}{\sqrt{2j+1}} \sum_{c=1}^{2j+1} \psi_{\gamma_1, j, a, c}[h_{\gamma_1}(A)] \psi_{\gamma_2, j, c, b}[h_{\gamma_2}(A)] \\ &= \frac{1}{\sqrt{2j+1}} \sum_{c=1}^{2j+1} \langle h | \gamma_1, j, a, c \rangle \langle h | \gamma_2, j, c, b \rangle. \end{aligned} \quad (130)$$

Equivalently, in Hilbert space notation,

$$|\gamma, j, a, b\rangle = \frac{1}{\sqrt{2j+1}} \sum_{c=1}^{2j+1} |\gamma_1, j, a, c\rangle \otimes |\gamma_2, j, c, b\rangle, \quad (131)$$

This expression is precisely a Schmidt decomposition for the state  $|\gamma, j, a, b\rangle$ . From it, the Schmidt coefficients are immediately read off as

$$\lambda_i = \frac{1}{\sqrt{2j+1}}, \quad i = 1, 2, \dots, 2j+1. \quad (132)$$

The entanglement entropy is then

$$S_A = S_B = -\sum_i \lambda_i^2 \log \lambda_i^2 = \log(2j+1). \quad (133)$$

Similarly, in LQG, one may ask whether there exists an operator whose eigenvalues directly correspond to entanglement entropy. More precisely, consider a state  $|\psi\rangle \in \mathcal{H} \subseteq \mathcal{H}_{\gamma_1} \otimes \mathcal{H}_{\gamma_2}$ . In this framework, there is a Noether charge  $Q$  originating from the Lagrangian such that [79]:

$$\widehat{\int_{\gamma_A} Q} |\psi\rangle = \log(2j+1) |\psi\rangle, \quad (134)$$

which yields a result analogous to that obtained in the string case (123).

Since the computation of entanglement entropy in both the open string and the LQG pictures requires performing the Schmidt decomposition in an analogous configuration, and given that both the open string charge density and the Wilson line are oriented objects, it becomes natural to investigate deeper relations between string theory and LQG. To approach this issue, let us recall Wall's conjecture [38]. Consider two theories: the first is string theory in AdS, which is dual to  $N=4$  super Yang–Mills theory; the second is LQG. If the LQG description is obtained through the quantization of AdS gravity, then it also admits a CFT dual. These two CFTs—the “stringy CFT” and the “LQG CFT”—can in principle become strongly entangled, thereby giving rise to a wormhole geometry. The wormhole throat thus unifies string theory and LQG, suggesting that the two frameworks are different descriptions of the same underlying theory.

Building on our earlier observations, we can refine this conjecture. Specifically, by considering the Schmidt decomposition of the open string charge density and the LQG Wilson line, one can split each system into two parts and then regroup half of them to form a new configuration, namely  $|\psi\rangle \in \mathcal{H} \subseteq \mathcal{H}_{\text{string}_1} \otimes \mathcal{H}_{\gamma_2}$ . Since both descriptions share the same quantized wormhole horizon, and the oriented open strings can connect to the oriented Wilson lines at the same points on the horizon, the two theories must coincide on the wormhole throat. This new perspective provides a concrete bridge between the string and LQG pictures through the language of entanglement, as illustrated in figure (20).

## 6 Conclusion and discussion

In this paper, we began with the entanglement entropy  $S_{\text{vN}}$  of a  $\text{CFT}_2$ . Utilizing this quantity and the RT prescription, we constructed Synge's world function  $\Omega(X, X') = 8G_N^2 S_{\text{vN}}^2$  in the bulk of  $\text{AdS}_3$ , corresponding to the square of the geodesic length between bulk points  $X$  and  $X'$ . Since both  $X$  and  $X'$  were boundary-determined bulk points fixed by the entangling regions in the CFT, they could be parameterized by the coordinates  $(\tau, \sigma)$  of the entangling regions of  $\text{CFT}_2$ . When the entangling regions varied, the entanglement entropy and its dual geodesic effectively generated a two-dimensional surface in the bulk, described by an embedding function  $X^\mu(\tau, \sigma)$ . Based on this observation, we proposed an action for entanglement entropy constructed from  $\Omega(X, X')$  and parameterized by  $(\tau, \sigma)$ . This action described the dynamics of this two-parameter family of geodesics. In the near-coincidence limit and employing RNC, the action reduced to a Polyakov-type string worldsheet action for the small separation field  $\hat{X}^a$ , with higher-order corrections. Requiring conformal symmetry of the worldsheet theory led to consistency conditions on the background fields, interpreted as the equations of motion for massless

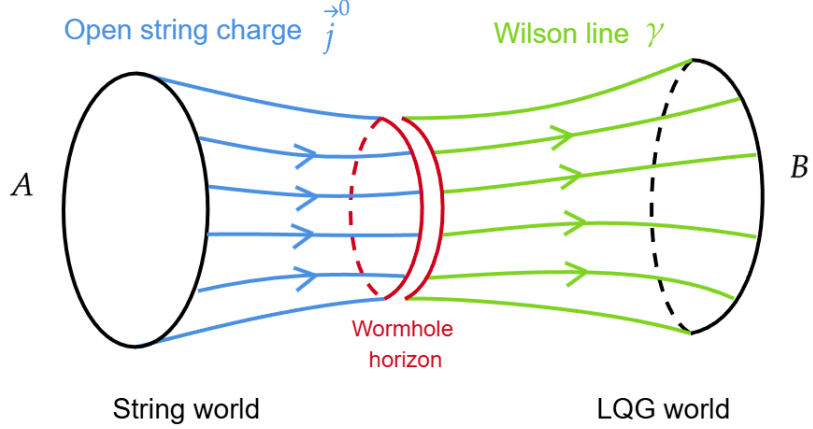


Figure 20: This picture illustrates the holographic dual of the Hilbert space  $\mathcal{H} \subseteq \mathcal{H}_{string} \otimes \mathcal{H}_{LQG}$ , under the assumption that one day AdS gravity can be quantized within the framework of LQG. The left part represents half of the BTZ wormhole, characterized by the open string charge density discussed previously in figure (13). The right part arises from the LQG construction, which can be obtained in a manner analogous to string theory, as suggested by the correspondence shown in figure (19). In this way, half of the Wilson line states can also be interpreted as constituting half of the wormhole. It is then natural to glue these two halves together along the horizon to form a new wormhole, with open strings and Wilson lines meeting at the same points on the horizon. The resulting theory therefore admits two equivalent descriptions: one in terms of string theory, and the other in terms of LQG.

closed string modes—namely, the gravitational field equations. Since  $\Omega(X, X')$  was constructed in  $AdS_3$ , the resulting equations admitted  $AdS_3$  as a solution. This consistency required the inclusion of an additional antisymmetric background field—the Kalb–Ramond field—and the dilaton field. This insight suggested that a corresponding quantity must also exist in the entanglement entropy picture.

Because entanglement entropy could be calculated from the symmetric spacetime metric, i.e., by computing the area of the RT surface, and since the antisymmetric Kalb–Ramond field entered the action on equal footing with the metric, there had to exist a way to compute entanglement entropy using the Kalb–Ramond field. The breakthrough came from bit threads, which are divergenceless and bounded vector fields perpendicular to the RT surface and provide an alternative formulation of entanglement entropy. In our case, the Kalb–Ramond field introduced the charge density vector  $\vec{j}^0$ , which is also divergenceless. To compare this charge density with bit threads, we embedded  $\vec{j}^0$  into the AdS background. This required employing methods from the study of string solitons, where  $\vec{j}^0$  played the role of a string source interacting with background fields. By considering multiple parallel string sources and taking the limits  $\kappa^2 = 8\pi G_N^{(3)} \rightarrow 0$  and  $g_s \ll 1$ , we successfully derived bit threads from the Kalb–Ramond charge density  $\vec{j}^0$ . This confirmed our conjecture that the antisymmetric Kalb–Ramond field could be used to compute entanglement entropy. Furthermore, this result allowed us to establish a concrete correspondence between the string worldsheet and the RT surface.

Exploiting this correspondence, we demonstrated that entanglement entropy could be computed within string theory: specifically, it was proportional to the number of open strings—each carrying Kalb–Ramond charge—that pierced the entangling surface. This result aligned with and extended previous studies connecting entanglement entropy to string-theoretic descriptions. Moreover, by applying open–closed string duality, the oriented open strings became closed strings winding around the horizon of the BTZ black hole. The corresponding closed string charge then captured the Bekenstein–Hawking entropy of the black hole. Based on this result, the ER=EPR correspondence could be reinterpreted from the perspective of string charge. The holographic disentanglement procedure, dual to the breaking of the wormhole horizon, could be interpreted as tachyon condensation driven by the decrease of the closed string charge  $Q$ . When  $Q = 0$ , the closed string became contractible in the compactified background, signifying that spacetime split into two disconnected components. This picture also provided a new realization of the Susskind–Uglum conjecture, with open–closed string duality, ER=EPR, and the Susskind–Uglum conjecture manifesting within the same configuration.

Finally, we discussed the possibility of quantizing entanglement entropy or the RT surface, since entanglement entropy could be realized as the number of strings crossing the RT surface. We also compared this result with entanglement entropy calculations in LQG. In both frameworks, the Schmidt decomposition could be employed to obtain entanglement entropy, implying that each system could be split into two parts and then regrouped to form a new configuration. This implication further refined Wall’s conjecture.

We conclude with the following remarks:

- In our work, after obtaining the action for the entanglement entropy, we reproduced the result using the bit thread method. This approach is well-defined and does not rely on the replica trick. Nevertheless, it remains important to understand how the replica trick could be implemented in our framework, and more specifically, how it can be realized directly on the string worldsheet. We believe our work provides a new perspective that may open the way toward such an approach.
- Based on recent developments of hyperbolic string vertices in closed string field theory (CSFT) [96, 97, 98, 99, 100, 101, 102, 103, 104], we have established a close relation between the entanglement wedge and hyperbolic string vertices [13, 14]. Specifically, the entanglement wedge cross-section (EWCS) corresponds to the boundary length  $L$  of the hyperbolic vertices  $\mathcal{V}_{g,n}(L)$ , where  $g$  denotes the genus and  $n$  the marked points of compact Riemann surfaces. Since  $\mathcal{V}_{g,n}(L)$  exactly solves the geometric master equation, complete knowledge of all string vertices  $\mathcal{V}_{g,n}(L)$  would in principle provide a full specification of string field theory. Moreover,  $\mathcal{V}_{g,n}(L)$  is uniquely determined by  $L$ . In our framework, there exists a parallel description for EWCS in terms of the string charge density. This observation suggests the possible existence of a string-charge formulation of string field theory.

**Acknowledgements** We would especially like to thank Aron Wall for reading the draft and providing valuable suggestions. We are deeply indebted to Xin Gao, Yongge Ma, Jun Nian, and Jia-Rui Sun

for helpful discussions. HW is grateful for the collaboration with Amr Ahmadain and Zihan Yan on a related project, which helped motivate this work. We are also grateful for the hospitality of Strings 2025 at New York University Abu Dhabi and of ICTP-AP, during which part of this work was completed.

HW is supported by NSFC Grant No.12105191. SY is supported by NSFC Grant No.12105031 and cstc2021jcyj-bshX0227.

## References

- [1] S. Ryu and T. Takayanagi, “Holographic derivation of entanglement entropy from AdS/CFT,” *Phys. Rev. Lett.* **96**, 181602 (2006) doi:10.1103/PhysRevLett.96.181602 [hep-th/0603001].
- [2] S. Ryu and T. Takayanagi, “Aspects of Holographic Entanglement Entropy,” *JHEP* **0608**, 045 (2006) doi:10.1088/1126-6708/2006/08/045 [hep-th/0605073].
- [3] V. E. Hubeny, M. Rangamani and T. Takayanagi, “A Covariant holographic entanglement entropy proposal,” *JHEP* **0707**, 062 (2007) doi:10.1088/1126-6708/2007/07/062 [arXiv:0705.0016 [hep-th]].
- [4] T. Faulkner, A. Lewkowycz and J. Maldacena, “Quantum corrections to holographic entanglement entropy,” *JHEP* **11**, 074 (2013) doi:10.1007/JHEP11(2013)074 [arXiv:1307.2892 [hep-th]].
- [5] N. Engelhardt and A. C. Wall, “Quantum Extremal Surfaces: Holographic Entanglement Entropy beyond the Classical Regime,” *JHEP* **01**, 073 (2015) doi:10.1007/JHEP01(2015)073 [arXiv:1408.3203 [hep-th]].
- [6] G. Penington, “Entanglement Wedge Reconstruction and the Information Paradox,” *JHEP* **09**, 002 (2020) doi:10.1007/JHEP09(2020)002 [arXiv:1905.08255 [hep-th]].
- [7] A. Almheiri, N. Engelhardt, D. Marolf and H. Maxfield, “The entropy of bulk quantum fields and the entanglement wedge of an evaporating black hole,” *JHEP* **12**, 063 (2019) doi:10.1007/JHEP12(2019)063 [arXiv:1905.08762 [hep-th]].
- [8] A. Almheiri, T. Hartman, J. Maldacena, E. Shaghoulian and A. Tajdini, “The entropy of Hawking radiation,” *Rev. Mod. Phys.* **93**, no.3, 035002 (2021) doi:10.1103/RevModPhys.93.035002 [arXiv:2006.06872 [hep-th]].
- [9] L. Susskind and J. Uglum, “Black hole entropy in canonical quantum gravity and superstring theory,” *Phys. Rev. D* **50**, 2700-2711 (1994) doi:10.1103/PhysRevD.50.2700 [arXiv:hep-th/9401070 [hep-th]].
- [10] A. Ahmadain and A. C. Wall, “Off-shell strings I: S-matrix and action,” *SciPost Phys.* **17**, no.1, 005 (2024) doi:10.21468/SciPostPhys.17.1.005 [arXiv:2211.08607 [hep-th]].

- [11] A. Ahmadain and A. C. Wall, “Off-shell strings II: Black hole entropy,” *SciPost Phys.* **17**, no.1, 006 (2024) doi:10.21468/SciPostPhys.17.1.006 [arXiv:2211.16448 [hep-th]].
- [12] A. Ahmadain, A. Frenkel and A. C. Wall, “A Background-Independent Closed String Action at Tree Level,” [arXiv:2410.11938 [hep-th]].
- [13] P. Wang, H. Wu and H. Yang, “Connections between reflected entropies and hyperbolic string vertices,” *JHEP* **05**, 127 (2022) doi:10.1007/JHEP05(2022)127 [arXiv:2112.09503 [hep-th]].
- [14] X. Jiang, H. Wu and H. Yang, “String scattering and evolution of a Ryu-Takayanagi surface,” *Phys. Rev. D* **111**, no.2, 026021 (2025) doi:10.1103/PhysRevD.111.026021 [arXiv:2408.12495 [hep-th]].
- [15] T. Takayanagi and K. Umemoto, “Entanglement of purification through holographic duality,” *Nature Phys.* **14**, no.6, 573-577 (2018) doi:10.1038/s41567-018-0075-2 [arXiv:1708.09393 [hep-th]].
- [16] S. Dutta and T. Faulkner, “A canonical purification for the entanglement wedge cross-section,” *JHEP* **03**, 178 (2021) doi:10.1007/JHEP03(2021)178 [arXiv:1905.00577 [hep-th]].
- [17] A. Sen and B. Zwiebach, “Quantum background independence of closed string field theory,” *Nucl. Phys. B* **423**, 580 (1994) doi:10.1016/0550-3213(94)90145-7 [hep-th/9311009].
- [18] A. Sen and B. Zwiebach, “Background independent algebraic structures in closed string field theory,” *Commun. Math. Phys.* **177**, 305 (1996) doi:10.1007/BF02101895 [hep-th/9408053].
- [19] N. Bao, H. Geng and Y. Jiang, “Ryu-Takayanagi formula for multi-boundary black holes from 2D large-c CFT ensemble,” *JHEP* **10**, 042 (2025) doi:10.1007/JHEP10(2025)042 [arXiv:2504.12388 [hep-th]].
- [20] A. Dabholkar, “Strings on a cone and black hole entropy,” *Nucl. Phys. B* **439**, 650-664 (1995) doi:10.1016/0550-3213(95)00050-3 [arXiv:hep-th/9408098 [hep-th]].
- [21] A. Dabholkar, “Quantum Entanglement in String Theory,” [arXiv:2207.03624 [hep-th]].
- [22] D. A. Lowe and A. Strominger, “Strings near a Rindler or black hole horizon,” *Phys. Rev. D* **51**, 1793-1799 (1995) doi:10.1103/PhysRevD.51.1793 [arXiv:hep-th/9410215 [hep-th]].
- [23] S. He, T. Numasawa, T. Takayanagi and K. Watanabe, “Notes on Entanglement Entropy in String Theory,” *JHEP* **05**, 106 (2015) doi:10.1007/JHEP05(2015)106 [arXiv:1412.5606 [hep-th]].
- [24] E. Witten, “Open Strings On The Rindler Horizon,” *JHEP* **01**, 126 (2019) doi:10.1007/JHEP01(2019)126 [arXiv:1810.11912 [hep-th]].
- [25] V. Balasubramanian and O. Parrikar, “Remarks on entanglement entropy in string theory,” *Phys. Rev. D* **97**, no.6, 066025 (2018) doi:10.1103/PhysRevD.97.066025 [arXiv:1801.03517 [hep-th]].
- [26] U. Naseer, “Entanglement Entropy in Closed String Theory,” [arXiv:2002.12148 [hep-th]].

- [27] J. L. Synge, editor. “Relativity: The General theory,” 1960.
- [28] E. Poisson, A. Pound and I. Vega, “The Motion of point particles in curved spacetime,” *Living Rev. Rel.* **14**, 7 (2011) doi:10.12942/lrr-2011-7 [arXiv:1102.0529 [gr-qc]].
- [29] C. G. Callan, Jr., E. J. Martinec, M. J. Perry and D. Friedan, “Strings in Background Fields,” *Nucl. Phys. B* **262**, 593-609 (1985) doi:10.1016/0550-3213(85)90506-1
- [30] A. Dabholkar, G. W. Gibbons, J. A. Harvey and F. Ruiz Ruiz, “Superstrings and Solitons,” *Nucl. Phys. B* **340**, 33-55 (1990) doi:10.1016/0550-3213(90)90157-9
- [31] A. Sen, “Macroscopic charged heterotic string,” *Nucl. Phys. B* **388**, 457-473 (1992) doi:10.1016/0550-3213(92)90622-I [arXiv:hep-th/9206016 [hep-th]].
- [32] M. J. Duff, R. R. Khuri and J. X. Lu, “String solitons,” *Phys. Rept.* **259**, 213-326 (1995) doi:10.1016/0370-1573(95)00002-X [arXiv:hep-th/9412184 [hep-th]].
- [33] M. Freedman and M. Headrick, “Bit threads and holographic entanglement,” *Commun. Math. Phys.* **352**, no.1, 407-438 (2017) doi:10.1007/s00220-016-2796-3 [arXiv:1604.00354 [hep-th]].
- [34] H. Casini, M. Huerta and R. C. Myers, “Towards a derivation of holographic entanglement entropy,” *JHEP* **05**, 036 (2011) doi:10.1007/JHEP05(2011)036 [arXiv:1102.0440 [hep-th]].
- [35] R. Espíndola, A. Guijosa and J. F. Pedraza, “Entanglement Wedge Reconstruction and Entanglement of Purification,” *Eur. Phys. J. C* **78**, no.8, 646 (2018) doi:10.1140/epjc/s10052-018-6140-2 [arXiv:1804.05855 [hep-th]].
- [36] S. Caccioli, F. Gentile, D. Seminara and E. Tonni, “Holographic thermal entropy from geodesic bit threads,” *JHEP* **07**, 088 (2024) doi:10.1007/JHEP07(2024)088 [arXiv:2403.03930 [hep-th]].
- [37] W. Donnelly and G. Wong, “Entanglement branes in a two-dimensional string theory,” *JHEP* **09**, 097 (2017) doi:10.1007/JHEP09(2017)097 [arXiv:1610.01719 [hep-th]].
- [38] A. C. Wall, “What if Quantum Gravity is ”just” Quantum Information Theory?,” [arXiv:2310.02958 [gr-qc]].
- [39] D. Tong, “String Theory,” [arXiv:0908.0333 [hep-th]].
- [40] J. Cardy and E. Tonni, “Entanglement hamiltonians in two-dimensional conformal field theory,” *J. Stat. Mech.* **1612**, no.12, 123103 (2016) doi:10.1088/1742-5468/2016/12/123103 [arXiv:1608.01283 [cond-mat.stat-mech]].
- [41] X. Jiang, P. Wang, H. Wu and H. Yang, “Alternative to purification in conformal field theory,” *Phys. Rev. D* **111**, no.2, L021902 (2025) doi:10.1103/PhysRevD.111.L021902 [arXiv:2406.09033 [hep-th]].

- [42] X. Jiang, P. Wang, H. Wu and H. Yang, “Mixed state entanglement entropy in CFT,” *JHEP* **09**, 133 (2025) doi:10.1007/JHEP09(2025)133 [arXiv:2501.08198 [hep-th]].
- [43] D. Basu, H. Parihar, V. Raj and G. Sengupta, “Entanglement negativity, reflected entropy, and anomalous gravitation,” *Phys. Rev. D* **105**, no.8, 086013 (2022) [erratum: *Phys. Rev. D* **105**, no.12, 129902 (2022)] doi:10.1103/PhysRevD.105.086013 [arXiv:2202.00683 [hep-th]].
- [44] Q. Wen and H. Zhong, “Covariant entanglement wedge cross-section, balanced partial entanglement and gravitational anomalies,” *SciPost Phys.* **13**, no.3, 056 (2022) doi:10.21468/SciPostPhys.13.3.056 [arXiv:2205.10858 [hep-th]].
- [45] X. Jiang, P. Wang, H. Wu and H. Yang, “How Einstein’s equations emerge from CFT2,” *Phys. Rev. D* **112**, no.8, 8 (2025) doi:10.1103/zg5x-34mn [arXiv:2410.19711 [hep-th]].
- [46] E. Hijano, P. Kraus, E. Perlmutter and R. Snively, “Semiclassical Virasoro blocks from  $AdS_3$  gravity,” *JHEP* **12**, 077 (2015) doi:10.1007/JHEP12(2015)077 [arXiv:1508.04987 [hep-th]].
- [47] E. Hijano, P. Kraus, E. Perlmutter and R. Snively, “Witten Diagrams Revisited: The  $AdS$  Geometry of Conformal Blocks,” *JHEP* **01**, 146 (2016) doi:10.1007/JHEP01(2016)146 [arXiv:1508.00501 [hep-th]].
- [48] H. Hirai, K. Tamaoka and T. Yokoya, “Towards Entanglement of Purification for Conformal Field Theories,” *PTEP* **2018**, no.6, 063B03 (2018) doi:10.1093/ptep/pty063 [arXiv:1803.10539 [hep-th]].
- [49] G. T. Horowitz and D. L. Welch, “Exact three-dimensional black holes in string theory,” *Phys. Rev. Lett.* **71**, 328-331 (1993) doi:10.1103/PhysRevLett.71.328 [arXiv:hep-th/9302126 [hep-th]].
- [50] J. M. Maldacena, “The Large  $N$  limit of superconformal field theories and supergravity,” *Adv. Theor. Math. Phys.* **2**, 231-252 (1998) doi:10.4310/ATMP.1998.v2.n2.a1 [arXiv:hep-th/9711200 [hep-th]].
- [51] N. Seiberg and E. Witten, “The  $D1 / D5$  system and singular CFT,” *JHEP* **04**, 017 (1999) doi:10.1088/1126-6708/1999/04/017 [arXiv:hep-th/9903224 [hep-th]].
- [52] M. R. Gaberdiel and R. Gopakumar, “Tensionless string spectra on  $AdS_3$ ,” *JHEP* **05**, 085 (2018) doi:10.1007/JHEP05(2018)085 [arXiv:1803.04423 [hep-th]].
- [53] L. Eberhardt, M. R. Gaberdiel and R. Gopakumar, “The Worldsheet Dual of the Symmetric Product CFT,” *JHEP* **04**, 103 (2019) doi:10.1007/JHEP04(2019)103 [arXiv:1812.01007 [hep-th]].
- [54] L. Eberhardt, M. R. Gaberdiel and R. Gopakumar, “Deriving the  $AdS_3/CFT_2$  correspondence,” *JHEP* **02**, 136 (2020) doi:10.1007/JHEP02(2020)136 [arXiv:1911.00378 [hep-th]].
- [55] L. Eberhardt, “A perturbative CFT dual for pure NS-NS  $AdS_3$  strings,” *J. Phys. A* **55**, no.6, 064001 (2022) doi:10.1088/1751-8121/ac47b2 [arXiv:2110.07535 [hep-th]].

- [56] B. Balthazar, A. Giveon, D. Kutasov and E. J. Martinec, “Asymptotically free  $\text{AdS}_3/\text{CFT}_2$ ,” JHEP **01**, 008 (2022) doi:10.1007/JHEP01(2022)008 [arXiv:2109.00065 [hep-th]].
- [57] E. J. Martinec, “A defect in  $\text{AdS}_3/\text{CFT}_2$  duality,” JHEP **06**, 024 (2022) doi:10.1007/JHEP06(2022)024 [arXiv:2201.04218 [hep-th]].
- [58] Z. f. Yu and C. Peng, “Correlators of long strings on  $\text{AdS}_3 \times S^3 \times T^4$ ,” JHEP **01**, 017 (2025) doi:10.1007/JHEP01(2025)017 [arXiv:2408.16712 [hep-th]].
- [59] Z. f. Yu, “On the CFT dual of superstring on  $\text{AdS}_3$ ,” [arXiv:2504.20227 [hep-th]].
- [60] D. Kutasov and N. Seiberg, “More comments on string theory on  $\text{AdS}(3)$ ,” JHEP **04**, 008 (1999) doi:10.1088/1126-6708/1999/04/008 [arXiv:hep-th/9903219 [hep-th]].
- [61] A. Giveon, D. Kutasov and N. Seiberg, “Comments on string theory on  $\text{AdS}(3)$ ,” Adv. Theor. Math. Phys. **2**, 733-782 (1998) doi:10.4310/ATMP.1998.v2.n4.a3 [arXiv:hep-th/9806194 [hep-th]].
- [62] J. de Boer, H. Ooguri, H. Robins and J. Tannenhauser, “String theory on  $\text{AdS}(3)$ ,” JHEP **12**, 026 (1998) doi:10.1088/1126-6708/1998/12/026 [arXiv:hep-th/9812046 [hep-th]].
- [63] J. M. Maldacena and H. Ooguri, “Strings in  $\text{AdS}(3)$  and  $\text{SL}(2, \mathbb{R})$  WZW model 1.: The Spectrum,” J. Math. Phys. **42**, 2929-2960 (2001) doi:10.1063/1.1377273 [arXiv:hep-th/0001053 [hep-th]].
- [64] J. M. Maldacena, H. Ooguri and J. Son, “Strings in  $\text{AdS}(3)$  and the  $\text{SL}(2, \mathbb{R})$  WZW model. Part 2. Euclidean black hole,” J. Math. Phys. **42**, 2961-2977 (2001) doi:10.1063/1.1377039 [arXiv:hep-th/0005183 [hep-th]].
- [65] J. M. Maldacena and H. Ooguri, “Strings in  $\text{AdS}(3)$  and the  $\text{SL}(2, \mathbb{R})$  WZW model. Part 3. Correlation functions,” Phys. Rev. D **65**, 106006 (2002) doi:10.1103/PhysRevD.65.106006 [arXiv:hep-th/0111180 [hep-th]].
- [66] C. A. Agón, E. Cáceres and J. F. Pedraza, “Bit threads, Einstein’s equations and bulk locality,” JHEP **01**, 193 (2021) doi:10.1007/JHEP01(2021)193 [arXiv:2007.07907 [hep-th]].
- [67] C. A. Agón and J. F. Pedraza, “Quantum bit threads and holographic entanglement,” JHEP **02**, 180 (2022) doi:10.1007/JHEP02(2022)180 [arXiv:2105.08063 [hep-th]].
- [68] M. Kleban, A. E. Lawrence and S. H. Shenker, “Closed strings from nothing,” Phys. Rev. D **64**, 066002 (2001) doi:10.1103/PhysRevD.64.066002 [arXiv:hep-th/0012081 [hep-th]].
- [69] J. X. Lu, “Branes in String/M-Theory,” Commun. Theor. Phys. **77**, no.9, 097001 (2025) doi:10.1088/1572-9494/adcc02 [arXiv:2502.11575 [hep-th]].
- [70] A. Strominger and C. Vafa, “Microscopic origin of the Bekenstein-Hawking entropy,” Phys. Lett. B **379**, 99-104 (1996) doi:10.1016/0370-2693(96)00345-0 [arXiv:hep-th/9601029 [hep-th]].

- [71] C. G. Callan and J. M. Maldacena, “D-brane approach to black hole quantum mechanics,” *Nucl. Phys. B* **472**, 591-610 (1996) doi:10.1016/0550-3213(96)00225-8 [arXiv:hep-th/9602043 [hep-th]].
- [72] J. M. Maldacena and A. Strominger, “AdS(3) black holes and a stringy exclusion principle,” *JHEP* **12**, 005 (1998) doi:10.1088/1126-6708/1998/12/005 [arXiv:hep-th/9804085 [hep-th]].
- [73] J. D. Bekenstein, “Black holes and entropy,” *Phys. Rev. D* **7**, 2333-2346 (1973) doi:10.1103/PhysRevD.7.2333
- [74] A. C. Wall, “A proof of the generalized second law for rapidly changing fields and arbitrary horizon slices,” *Phys. Rev. D* **85**, 104049 (2012) [erratum: *Phys. Rev. D* **87**, no.6, 069904 (2013)] doi:10.1103/PhysRevD.85.104049 [arXiv:1105.3445 [gr-qc]].
- [75] R. H. Brandenberger and C. Vafa, “Superstrings in the Early Universe,” *Nucl. Phys. B* **316**, 391-410 (1989) doi:10.1016/0550-3213(89)90037-0
- [76] A. A. Tseytlin and C. Vafa, “Elements of string cosmology,” *Nucl. Phys. B* **372**, 443-466 (1992) doi:10.1016/0550-3213(92)90327-8 [arXiv:hep-th/9109048 [hep-th]].
- [77] T. Battefeld and S. Watson, “String gas cosmology,” *Rev. Mod. Phys.* **78**, 435-454 (2006) doi:10.1103/RevModPhys.78.435 [arXiv:hep-th/0510022 [hep-th]].
- [78] C. A. Agón, J. De Boer and J. F. Pedraza, “Geometric Aspects of Holographic Bit Threads,” *JHEP* **05**, 075 (2019) doi:10.1007/JHEP05(2019)075 [arXiv:1811.08879 [hep-th]].
- [79] W. Donnelly, “Entanglement entropy in loop quantum gravity,” *Phys. Rev. D* **77**, 104006 (2008) doi:10.1103/PhysRevD.77.104006 [arXiv:0802.0880 [gr-qc]].
- [80] P. Wang, H. Wu and H. Yang, “Fixing the  $AdS_3$  metric from pure state entanglement entropies of  $CFT_2$ ,” *Chin. Phys. C* **49**, no.4, 045105 (2025) doi:10.1088/1674-1137/ada960 [arXiv:1710.08448 [hep-th]].
- [81] P. Wang, H. Wu and H. Yang, “Fixing three dimensional geometries from entanglement entropies of  $CFT_2$  \*,” *Chin. Phys. C* **49**, no.2, 025106 (2025) doi:10.1088/1674-1137/ad93b8 [arXiv:1809.01355 [hep-th]].
- [82] P. Wang, H. Wu and H. Yang, “Fix the dual geometries of  $T\bar{T}$  deformed  $CFT_2$  and highly excited states of  $CFT_2$ ,” *Eur. Phys. J. C* **80**, no.12, 1117 (2020) doi:10.1140/epjc/s10052-020-08680-7 [arXiv:1811.07758 [hep-th]].
- [83] B. Zwiebach, “A first course in string theory,” Cambridge University Press, 2006, ISBN 978-0-521-83143-7, 978-0-511-20757-0
- [84] T. Hartman, “Lectures on Quantum Gravity and Black Holes.”

- [85] N. Callebaut, “Entanglement in Conformal Field Theory and Holography,” *Lect. Notes Phys.* **1022**, 239-271 (2023) doi:10.1007/978-3-031-42096-2\_10 [arXiv:2303.16827 [hep-th]].
- [86] J. M. Maldacena, “Eternal black holes in anti-de Sitter,” *JHEP* **04**, 021 (2003) doi:10.1088/1126-6708/2003/04/021 [arXiv:hep-th/0106112 [hep-th]].
- [87] M. Banados, C. Teitelboim and J. Zanelli, “The Black hole in three-dimensional space-time,” *Phys. Rev. Lett.* **69**, 1849-1851 (1992) doi:10.1103/PhysRevLett.69.1849 [arXiv:hep-th/9204099 [hep-th]].
- [88] T. Azeyanagi, T. Nishioka and T. Takayanagi, “Near Extremal Black Hole Entropy as Entanglement Entropy via AdS(2)/CFT(1),” *Phys. Rev. D* **77**, 064005 (2008) doi:10.1103/PhysRevD.77.064005 [arXiv:0710.2956 [hep-th]].
- [89] S. Ying, “Probing black hole entropy via entanglement,” [arXiv:2505.08012 [hep-th]].
- [90] A. Adams, X. Liu, J. McGreevy, A. Saltman and E. Silverstein, “Things fall apart: Topology change from winding tachyons,” *JHEP* **10**, 033 (2005) doi:10.1088/1126-6708/2005/10/033 [arXiv:hep-th/0502021 [hep-th]].
- [91] H. Geng, “Replica wormholes and entanglement islands in the Karch-Randall braneworld,” *JHEP* **01**, 063 (2025) doi:10.1007/JHEP01(2025)063 [arXiv:2405.14872 [hep-th]].
- [92] H. Geng, L. Y. Hung and Y. Jiang, “It from ETH: Multi-interval Entanglement and Replica Wormholes from Large- $c$  BCFT Ensemble,” [arXiv:2505.20385 [hep-th]].
- [93] A. Kundu, “Wormholes and holography: an introduction,” *Eur. Phys. J. C* **82**, no.5, 447 (2022) doi:10.1140/epjc/s10052-022-10376-z [arXiv:2110.14958 [hep-th]].
- [94] L. Susskind, “Strings, black holes and Lorentz contraction,” *Phys. Rev. D* **49**, 6606-6611 (1994) doi:10.1103/PhysRevD.49.6606 [arXiv:hep-th/9308139 [hep-th]].
- [95] A. Mousatov and E. Silverstein, “Recovering Infalling Information via String Spreading,” [arXiv:2002.12377 [hep-th]].
- [96] K. Costello and B. Zwiebach, “Hyperbolic string vertices,” *JHEP* **02**, 002 (2022) doi:10.1007/JHEP02(2022)002 [arXiv:1909.00033 [hep-th]].
- [97] M. Cho, “Open-closed Hyperbolic String Vertices,” *JHEP* **05**, 046 (2020) doi:10.1007/JHEP05(2020)046 [arXiv:1912.00030 [hep-th]].
- [98] A. H. Firat, “Hyperbolic three-string vertex,” *JHEP* **08**, 035 (2021) doi:10.1007/JHEP08(2021)035 [arXiv:2102.03936 [hep-th]].

- [99] H. Erbin, “String Field Theory: A Modern Introduction,” *Lect. Notes Phys.* **980**, 1-421 (2021) 2021, ISBN 978-3-030-65320-0, 978-3-030-65321-7 doi:10.1007/978-3-030-65321-7 [arXiv:2301.01686 [hep-th]].
- [100] H. Erbin and A. H. Firat, “Characterizing 4-string contact interaction using machine learning,” *JHEP* **04**, 016 (2024) doi:10.1007/JHEP04(2024)016 [arXiv:2211.09129 [hep-th]].
- [101] A. H. Firat, “Bootstrapping closed string field theory,” *JHEP* **05**, 186 (2023) doi:10.1007/JHEP05(2023)186 [arXiv:2302.12843 [hep-th]].
- [102] A. H. Firat, “Hyperbolic string tadpole,” *SciPost Phys.* **15**, no.6, 237 (2023) doi:10.21468/SciPostPhys.15.6.237 [arXiv:2306.08599 [hep-th]].
- [103] A. H. Firat, “String vertices for the large N limit,” *Nucl. Phys. B* **1000**, 116485 (2024) doi:10.1016/j.nuclphysb.2024.116485 [arXiv:2311.00747 [hep-th]].
- [104] A. H. Firat and N. Valdes-Meller, “Topological recursion for hyperbolic string field theory,” *JHEP* **11**, 005 (2024) doi:10.1007/JHEP11(2024)005 [arXiv:2409.02982 [hep-th]].